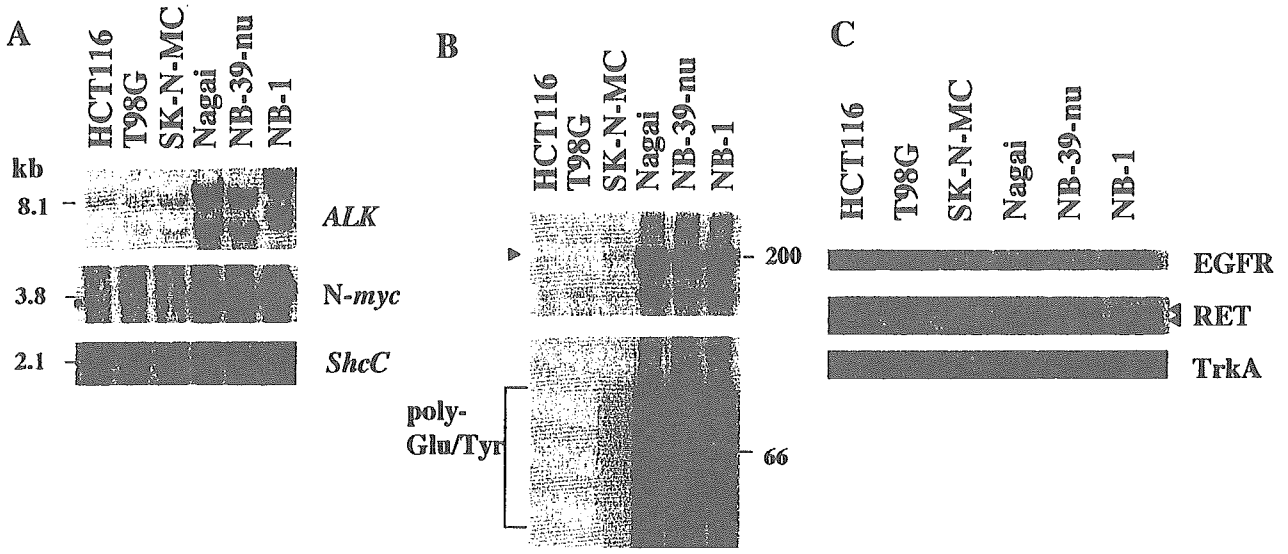

Figure 1. Marked gene amplification of the *ALK* locus and significant elevation of kinase activity of ALK in NB-39-nu, Nagai, and NB-1 cells. **A:** To detect ALK gene amplification, samples of 10 μg of DNA were digested with *Eco*RI. Fragments of about 2.5, 3.1, 6.1, and 8.1 kb were detected using the ^{32}P-labeled probe prepared as previously described.[27] Amplification of the N-*myc* gene was detected using the same filter re-hybridized with the probe for N-*myc*. As a control for the amounts of DNA, the same filter was re-hybridized with the probe for *ShcC*. **B:** *In vitro* kinase assay of ALK in neuroblastoma cells immunoprecipitated with αALK was performed as previously described.[27] Kinase reaction was performed without (**top panel**) or with (**bottom panel**) poly-Glu/Tyr (4:1) as exogenous substrates. Autophosphorylated ALK protein is marked by an **arrow**. Phosphorylated poly-Glu/Tyr is detected as smear indicated by the bracket. **C:** The expression patterns of other receptor tyrosine kinases in neuroblastoma cell lines. Each cell line was harvested, and about 30 μg of whole-cell lysates was subjected to Western blot analysis using the antibodies as indicated on the right. RET proteins are marked by **arrows**.

other types of solid tumor cell lines used as controls. *In vitro* kinase assay revealed outstanding ALK kinase activity in these three cell lines compared with other cells (Figure 1B), which is consistent with our previous study.[27] To examine whether overexpressed and activated ALK affects the expression of other RTKs in these cells, protein expression levels of RTKs, including EGFR, Ret, and TrkA, are compared with other cell lines. Significantly high levels of expression of EGFR and TrkA were observed in two of three cell lines overexpressing ALK (Figure 1C, top and bottom). Ret expression was commonly elevated in all three cell lines with activated ALK, especially in Nagai and NB-39-nu (Figure 1C, middle), consistent with previous study by Northern blotting.[32] Although it is unknown whether overexpression of these RTKs is related to overexpression of ALK, no obvious down-regulation of other RTKs was found in these *ALK*-amplified cell lines.

Inhibition of Activated ShcC, MAPKs, and Akt by Suppressing Activated ALK

To investigate the effect of suppressing the ALK expression level in *ALK*-amplified neuroblastoma cells using the RNAi technique, we synthesized two different RNA duplexes directed against nucleotide positions 153 to 171 and 399 to 417 within coding region *ALK* cDNA (ALK-siRNA1 and ALK-siRNA2, respectively). Because cotransfection of ALK-siRNA1 and ALK-siRNA2 was very effective in suppressing ALK expression, we performed all experiments presented here using a combination of two siRNAs, although similar results were obtained using only ALK-siRNA2. A sequence against the firefly luciferase gene (luc-siRNA) was used as a negative control. The expression of ALK protein is remarkably elevated in NB-39-nu and Nagai compared with other neuroblastoma cell lines, such as SK-M-MC (Figure 2A), caused by gene amplification.[27] The RNA duplexes were transfected into NB-39-nu cells with *ALK* gene amplification and SK-N-MC cells containing only a single copy of the *ALK* gene. We also tried to introduce ALK-siRNAs in several different neuroblastoma cell lines with or without *ALK* amplification in addition to NB-39-nu and SK-N-MC cells, resulting in partial or no reduction of ALK expression presumably due to the unsuccessful introduction in those cells. Therefore, we decided to use these two cell lines to perform further analysis of the effect of ALK knockdown by RNAi technique. RT-PCR analysis revealed that ALK mRNA level was reduced in both NB-39-nu cells and SK-N-MC cells treated with ALK-siRNAs, not in the cells treated with luc-siRNA and s-siRNA (Figure 2B). Both expression and phosphorylation of ALK kinase were significantly suppressed in the NB-39-nu cells treated with ALK-siRNAs compared with a mock-transfection control or cells treated with luc-siRNA (Figure 2C). In these cells, phosphorylation of ShcC was also suppressed despite the unchanged total amount of ShcC (Figure 2C), demonstrating that ShcC is a potent substrate of activated ALK kinase and that activation of ALK is actually responsible for the hyperphosphorylation of ShcC in these cancer cells. While the expression of downstream molecules, such as p44/42 MAPKs and Akt, was not affected by ALK-siRNAs, phosphorylation of these molecules was markedly reduced (Figure 2C). These results suggest that the Ras-MAPK pathway and the phosphatidylinositol 3-kinase/Akt pathway are dominantly regulated by activated ALK kinase in these cells. Interestingly, in SK-N-MC cells treated with ALK-siRNAs, phosphorylation levels of ShcC, p44/42 MAPKs, and Akt were not affected by

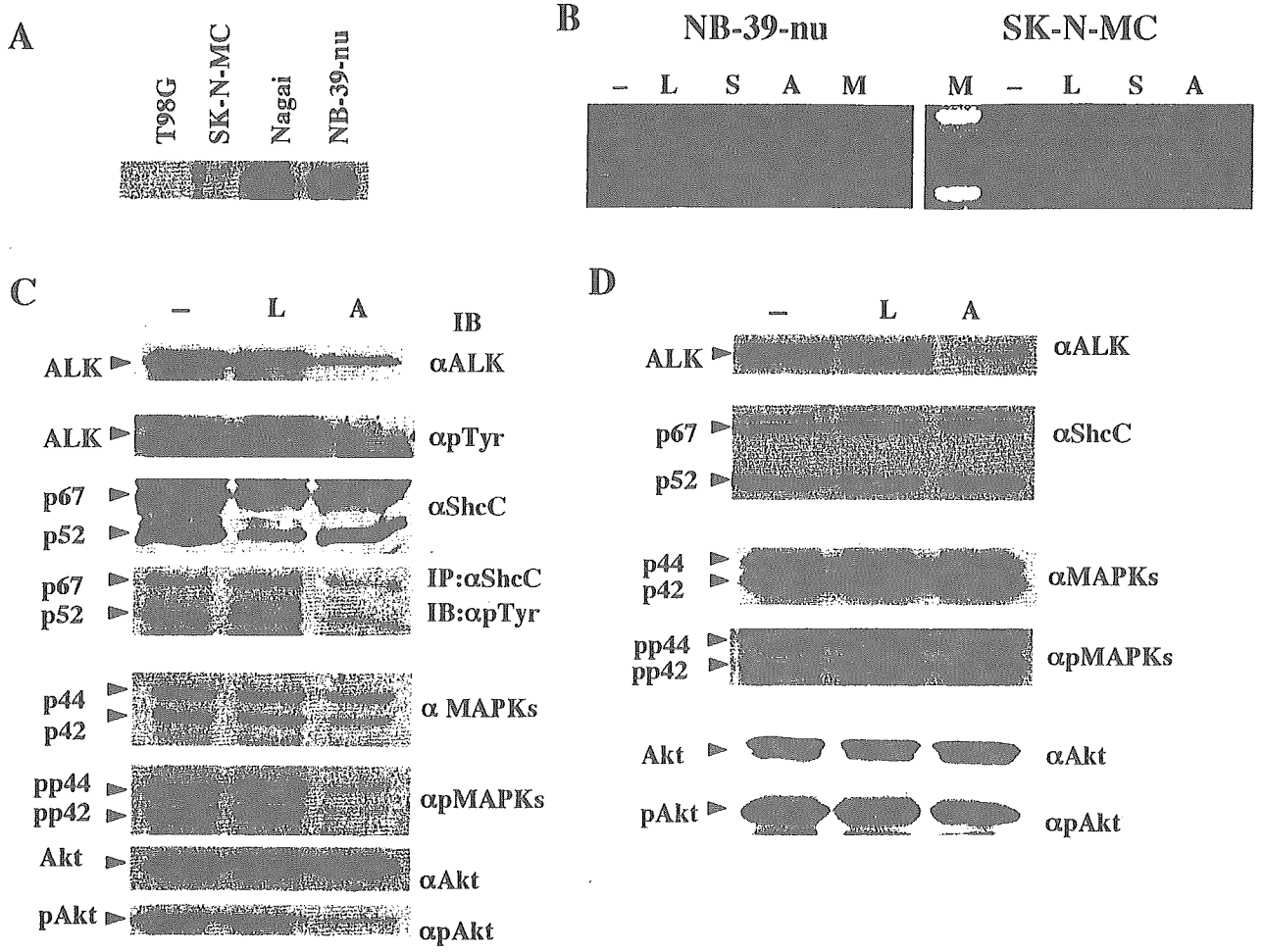

Figure 2. Suppression of ALK expression by siRNAs and changes in downstream molecules NB-39-nu cells and SK-N-MC cells. **A:** Expression levels of ALK protein in neuroblastoma cell lines including NB-39-nu and SK-N-MC. Each cell line was harvested, and about 30 μg of whole-cell lysates was subjected to Western blot analysis using αALK. **B:** mRNA levels of *Alk* in NB-39-nu cells. The cells were lysed at 84 hours after transfection and analyzed by RT-PCR. –, mock transfection; L, cells treated with luc-siRNA; S, cells treated with s-siRNA; A, cells treated with ALK-siRNAs; M, marker. **C:** NB-39-nu cells were harvested 84 hours after transfection. About 10 μg of whole-cell lysates or 250 μg of lysates immunoprecipitated with αShcC was subjected to Western blot analysis using the antibodies as indicated on the right. –, mock transfection; L, cells treated with luc-siRNA; A, cells treated with ALK-siRNAs. **D:** SK-N-MC cells were harvested 48 hours after transfection. About 10 μg of whole-cell lysates was subjected to Western blot analysis using the antibodies as indicated on the right. Bands of ShcC are marked by **arrows**. –, mock transfection; L, cells treated with luc-siRNA; A, cells treated with ALK-siRNAs.

ALK-siRNAs despite further suppression of the basal ALK expression level (Figure 2D), indicating that these pathways are not under the control of ALK in SK-N-MC cells.

Induction of Apoptosis by Suppression of Activated ALK

At 84 hours after transfection, apoptotic morphological changes, such as cell rounding, cytoplasmic blebbing, and irregularities of shape, were observed in NB-39-nu cells treated with ALK-siRNAs, whereas no significant changes were seen in the mock-transfected cells or in the luc-siRNA and the s-siRNA treated cells (Figure 3A). These morphological changes were not observed in SK-N-MC cells treated with ALK-siRNAs (data not shown). At 90 hours after transfection, NB-39-nu cells treated with ALK-siRNAs started to detach from the dish due to cell death.

To examine the localization of expression of ALK kinase, we performed double staining by anti-ALK antibody and TOTO-3, which stains the nucleus, in several neuroblastic cell lines. As shown in Figure 1D, unexpectedly, ALK protein overexpressed in NB-39-nu cells is localized in both membrane and cytoplasm. ALK staining was very weak in cell lines such as YT-nu and SK-N-MC with one copy of the *ALK* gene, however, its localization appeared to be the same as in NB-39-nu (data not shown). It was observed that the expression of ALK was completely lost after the RNAi-induced suppression of ALK (Figure 3C, top). To confirm whether the cell death resulted from apoptosis, cells were also analyzed by immunofluorescent TUNEL staining in NB-39-nu cells. TUNEL staining was clearly positive in these cells at 84 hours after transfection (Figure 3C, middle), indicating that apoptosis was induced in NB-39-nu cells treated with ALK-siRNAs. No significant TUNEL staining was observed in the mock-transfected cells or the luc-siRNA treated cells. Finally, DNA fragmentation assay was performed to measure the endonuclease activity accompa-

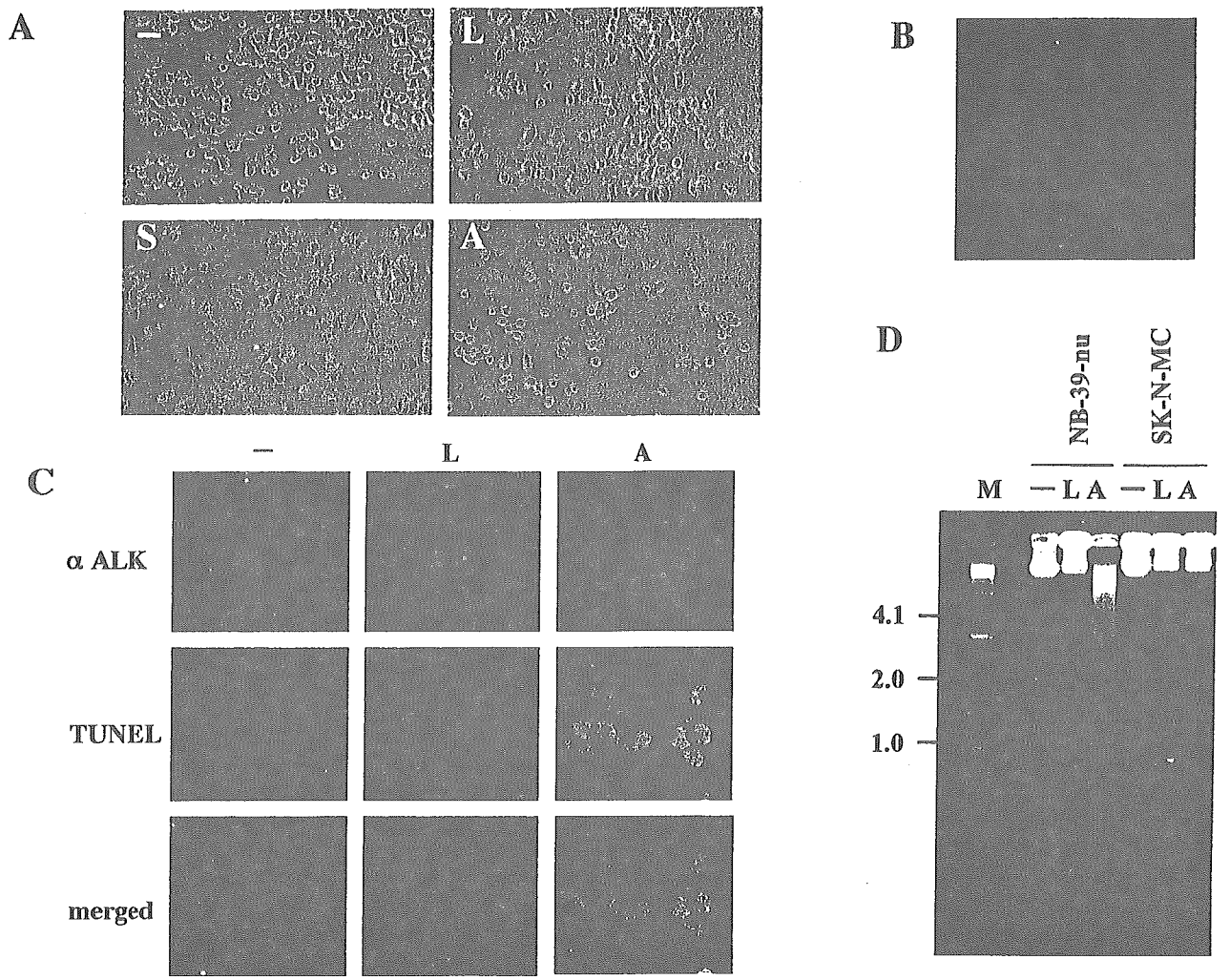

Figure 3. Induction of apoptosis in NB-39-nu cells treated with ALK-siRNAs. **A:** NB-39-nu cells on the dish were observed 84 hours after transfection under a light microscope. –, mock transfection; L, cells treated with luc-siRNA; S, cells treated with s-siRNA; A, cells treated with ALK-siRNAs. **B:** Cytoplasmic expression of ALK by immunocytostaining. The cells were stained for the expression of ALK (red) and apoptotic cells by TOTO-3 (blue). **C:** Cells on 24-well plates were fixed, and TUNEL assay was followed by staining with αALK (GST). The cells were stained for the expression of ALK (red) and apoptotic cells by TUNEL (green). –, mock transfection; L, cells treated with luc-siRNA; A, cells treated with ALK-siRNAs. **D:** DNA fragmentation assay in NB-39-nu cells and SK-N-MC cells treated with siRNAs. Genomic DNA was extracted 84 hours and 48 hours after transfection in NB-39-nu and in SK-N-MC, respectively. They were analyzed using electrophoresis. –, mock transfection; L, cells treated with luc-siRNA; A, cells treated with ALK-siRNAs; M, marker.

nied by apoptosis. The formation of significant DNA fragmentation was observed in the NB-39-nu cells but not in SK-N-MC cells treated with ALK-siRNAs (Figure 3D), indicating that cell apoptosis was induced through the suppression of ALK only in the NB-39-nu cells. This suggests that signaling pathways downstream of activated ALK dominantly regulate the survival of neuroblastoma cells with amplified ALK; therefore, the loss of ALK protein results in apoptotic changes to these cells.

Expression of ALK in Primary Neuroblastoma Tissues

Immunohistochemically, ALK was positively detected both in the cytoplasm of the neuroblastic cells and in the fine meshwork of neuropil of seven of nine tumors with favorable histology cases with nonamplified *N-myc* (FH&NA) (Figure 4, B and C). All seven unfavorable histology tumors (two UH&A tumors and five UH&NA tumors) were positive in the cytoplasm and/or in the fine meshwork of neuropil for ALK (Figure 4A). There was no correlation between the frequency or intensity of ALK-staining and histology of neuroblastoma tissues, showing majority of neuroblastoma samples showed a detectable amount of ALK. There was no significant staining using preimmune serum from the same rabbit as that for anti-ALK antibody (data not shown). Essentially the same results were obtained using a mouse monoclonal antibody against human ALK (ALK1: DAKO) (data not shown).

Amplification of the ALK Gene in Primary Neuroblastoma Tissues

It is essential to show whether ALK overexpression or gene amplification occurs in actual human neuroblastoma tissues in addition to neuroblastoma cell lines.

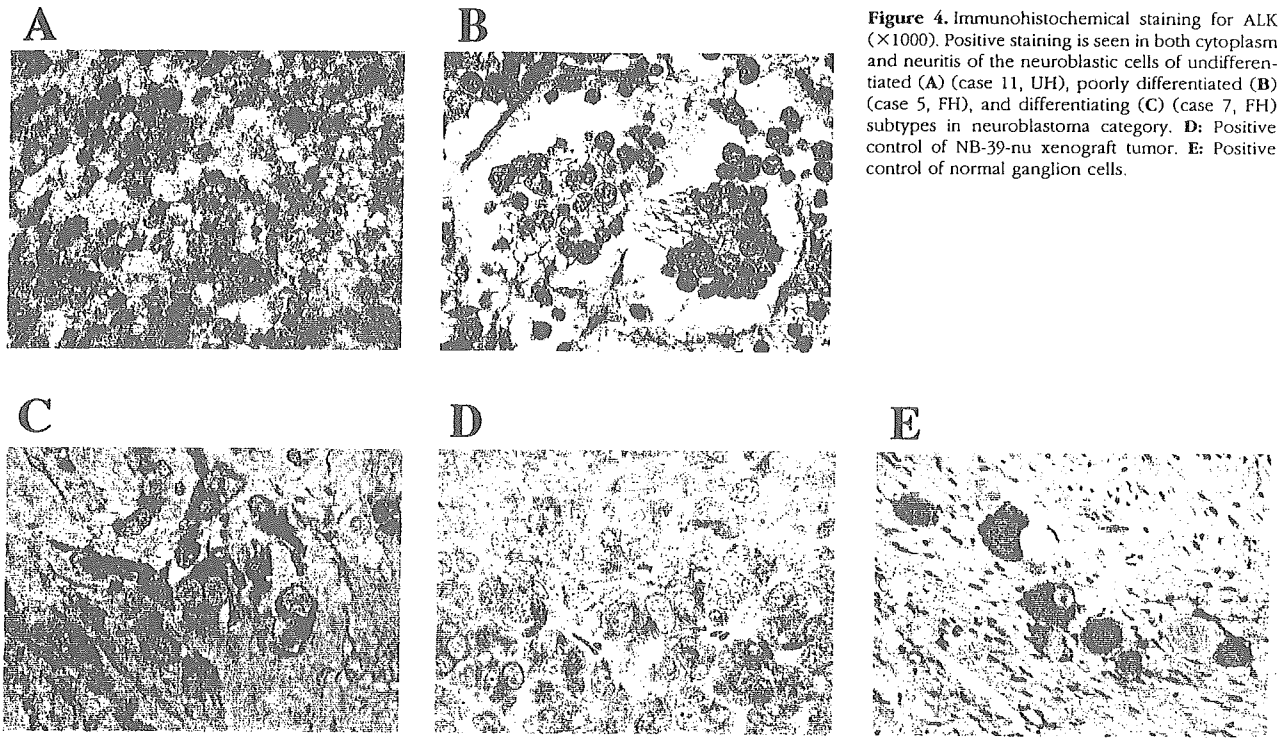

Figure 4. Immunohistochemical staining for ALK (×1000). Positive staining is seen in both cytoplasm and neuritis of the neuroblastic cells of undifferentiated (**A**) (case 11, UH), poorly differentiated (**B**) (case 5, FH), and differentiating (**C**) (case 7, FH) subtypes in neuroblastoma category. **D:** Positive control of NB-39-nu xenograft tumor. **E:** Positive control of normal ganglion cells.

Therefore, the mRNA amount of ALK kinase was first examined by RT-PCR on 32 primary neuroblastoma tissues (16 tissues with N-*myc* amplification and 16 tissues without N-*myc* amplification). Two of 32 cases showed slight elevation of *ALK* mRNA expression using several primer sets beyond the average expression level (data not shown).

To obtain more precise information about the copy numbers of *ALK*, we next analyzed the genomic DNAs of primary neuroblastoma tissues using Southern blot analysis. Whole purified DNA samples of tumors from 85 patients were examined. About the same number of N-*myc*-positive and N-*myc*-negative samples were collected to examine the relation between *Alk* and N-*myc* amplification. The intensities of signals on Southern blot membranes corresponding to the *ALK* gene and control *ShcC* gene, which is located on 9q22, were measured using a Molecular Imager FxPro (Bio-Rad), and the ratio of *ALK* signals to *ShcC* signals was calculated for each sample. Because more than 80% (70 samples) showed consistent ratios with each other in each experiment, these samples are treated as putative "single copy" controls. As several other samples showed apparently elevated intensity ratios, suggesting *ALK* amplification, relative copy numbers of *ALK* were calculated in comparison with average intensity ratios of putative single copy controls in each experiment. The results showed that there was significant *ALK* gene amplification in 8 of 85 patients (9.4%) (Figure 5). Seven of these eight cases, however, had only 1.8 to 3.0 copies of the *ALK* gene, suggesting a moderate gain of chromosomal focus rather than severe amplification. There was only one case that had outstanding amplification of ALK with approximately 10 copies. N-*myc* gene amplification was also detected in this case. The characteristics of the eight patients with *ALK* gain or amplification are shown in Table 1. Whereas seven of eight patients were classified as Stage III or IV (one as Stage III and six as Stage IV), the rest was classified as Stage I. The case with *ALK* amplification had N-*myc* amplification and was classified as Stage IV. Seven of eight patients were more than 1 year of age.

Discussion

Studies on ALK kinase demonstrate that activated ALK is involved in malignant tumor formation as forms of fusion proteins that force oligomerization of this kinase. We recently showed that the intact form of ALK protein is con-

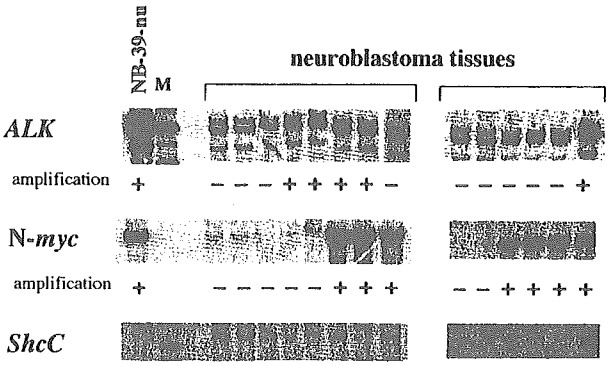

Figure 5. Detection of gene amplification of *ALK* and N-*myc* in primary neuroblastoma tissues. *ALK* was amplified in eight cases, and five of these eight cases are shown. The probe for *ALK* was removed from the filters, and the filters were re-hybridized in turn with other probes. Of eight cases with *ALK* amplification, N-*myc* amplification was detected in six cases and not detected in two cases. The probe for *ShcC* was used as a control for the amounts of DNA. M, marker.

stitutively activated by *ALK* gene amplification in three neuroblastoma cell lines, indicating a novel mechanism of activation of ALK kinase in malignancies.[27] In this study, amplification of the *ALK* gene was detected in primary neuroblastoma tissues for the first time. This suggests that activated ALK kinase plays a real role in the pathophysiology of neuroblastoma, such as giving a more malignant phenotype to the tumors by perturbing signal transduction. Recently, Motegi et al[33] showed that ALK transmits both mitogenic and differentiation signals, and that the MAPK pathway plays an important role in these effects in SK-N-SH cells without *ALK* gene amplification. Together with the fact that activated ALK surpasses regulation by other RTKs in cell lines with *ALK* gene amplification,[27] our new results showing apoptotic changes caused by the suppression of activated ALK protein clearly demonstrate the dominant role of ALK kinase in the survival of the *ALK*-amplified type of neuroblastoma.

The frequency and copy numbers of gene amplification of ALK were significantly lower in neuroblastic tumors compared with neuroblastic cell lines. Remarkable amplification of the *ALK* gene was detected in 1 tumor tissue of 85 tumor samples examined. Three neuroblastoma cell lines with *ALK* amplification had more than 30 copies of *ALK*, whereas primary neuroblastoma containing *ALK* gene amplification had within a range of 2 to 10 copies. This may be due to underestimation of the copy number in the tumor cells because of contamination of stromal cells and lymphocytes into the tumor tissues.[34,35] There may also be a mechanism in which cells with a higher copy number of *ALK* become the major population during the establishment of cell lines because of their growth advantage. Immunohistochemical analysis demonstrated, however, universal cytoplasmic expression of ALK in a wide range of neuroblastoma tumor samples, suggesting some transcriptional or posttranslational regulation of the ALK amount might exist in neuroblastoma cells. Although, due to the condition of the samples, we were unable to obtain information on the copy numbers of the *ALK* gene as for the samples used in the immunohistochemical analysis, further immunohistochemical screening may reveal neuroblastoma tissues with an outstanding amount of ALK protein because of gene amplification.

The N-*myc* gene was also amplified in this tumor and in all three cell lines with *ALK* amplification (NB-39-nu, Nagai, and NB-1). N-*myc* is located on 2p24.3 and *ALK* is on 2p23.2, suggesting that there is a tendency to synchronic amplification between N-*myc* and *ALK*. We were unable to conclude that there was an association between ALK amplification and prognosis mainly due to the limited number of positive samples and the short-term follow-up. Moreover, the *ALK* gene locus appears too far from the N-*myc* gene locus to be within a single amplicon. Further analysis in a greater number of samples with longer follow-up is necessary.

The activation of ALK results in hyperphosphorylation of ShcC in neuroblastoma cells, and NB-39-nu cells treated with ALK-siRNAs show suppressed tyrosine phosphorylation of ShcC, followed by apoptotic changes to these cells, suggesting that ShcC is a physiological substrate of the activated ALK kinase and that the ALK-ShcC pathway dominantly controls the survival of NB-39-nu cells even with the existence of other RTKs, such as EGFR, TrkA, and Ret. In neuronal cells, both ShcB (Sli/SCK) and ShcC (Rai/N-Shc) can bind activated RTKs, including the EGFR and Trk receptor.[36–39] Mice lacking both ShcB and ShcC exhibit a significant loss of sympathetic neurons, suggesting that ShcB and ShcC act in supporting sympathetic development and survival.[28] A recent study also showed that ShcC is a physiological substrate of Ret kinase and that it exerts a prosurvival function in neuronal cells.[40] Although high levels of TrkA expression correlate with a favorable outcome of neuroblastoma patients,[20] TrkA expression was significantly high in NB-39-nu and Nagai, which derive from tumors with a poor prognosis. This discrepancy may also be explained by the overwhelming control of cell survival by ALK kinase in these cell lines. Neuronal apoptosis is regulated through the action of critical protein kinase cascades, such as the phosphatidylinositol 3-kinase/Akt pathway and the Ras-MAPK pathway.[41,42] Apparently, neither pathway is properly controlled by EGF or nerve growth factor in NB-39-nu cells or Nagai cells.[27] Here, we also demonstrated that the suppression of activated ALK blocks MAPKs and Akt in these cells, resulting in apoptosis. On the other hand, the activity of MAPKs and Akt was not reduced by the suppression of a single copy of *ALK* in SK-N-MC cells. These results suggest that activation of ALK kinase completely remodeled the cellular signaling transduction pathways through ShcC so that cell survival entirely depended on signals originating from ALK kinase.

In conclusion, phosphorylation of several signaling molecules and cancer survival might be under the control of activated ALK kinase when gene amplification of ALK is as significant as in NB-39-nu cells, although the frequency of gene amplification in neuroblastoma tissues is not high. Cytoplasmic expression of ALK in neuroblastoma cells may suggest distinct function of this kinase in cell proliferation and survival. These findings further suggest that activated ALK kinase will be indispensable information for prognosis and treatment of neuroblastoma although the frequency is low.

References

1. Ullrich A, Schlessinger J: Signal transduction by receptors with tyrosine kinase activity. Cell 1990, 61:203–212
2. Heldin CH: Dimerization of cell surface receptors in signal transduction. Cell 1995, 80:213–223
3. Blume-Jensen P, Hunter T: Oncogenic kinase signalling. Nature 2001, 411:355–365
4. Pawson T: Protein modules and signalling networks. Nature 1995, 373:573–580
5. Kozlowski M, Larose L, Lee F, Le DM, Rottapel R, Siminovitch KA: SHP-1 binds and negatively modulates the c-Kit receptor by interaction with tyrosine 569 in the c-Kit juxtamembrane domain. Mol Cell Biol 1998, 18:2089–2099
6. Morris SW, Kirstein MN, Valentine MB, Dittmer KG, Shapiro DN, Saltman DL, Look AT: Fusion of a kinase gene ALK, to a nucleolar protein gene NPM, in non-Hodgkin's lymphoma. Science 1994, 263:1281–1284

7. Shiota M, Fujimoto J, Semba T, Satoh H, Yamamoto T, Mori S: Hyperphosphorylation of a novel 80 kDa protein-tyrosine kinase similar to Ltk in a human Ki-1 lymphoma cell line, AMS3. Oncogene 1994, 9:1567–1574
8. Bridge JA, Kanamori M, Ma Z, Pickering D, Hill DA, Lydiatt W, Lui MY, Colleoni GW, Antonescu CR, Ladanyi M, Morris SW: Fusion of the ALK gene to the clathrin heavy chain gene, CLTC, in inflammatory myofibroblastic tumor. Am J Pathol 2001, 159:411–415
9. Iwahara T, Fujimoto J, Wen D, Cupples R, Bucay N, Arakawa T, Mori S, Ratzkin B, Yamamoto T: Molecular characterization of ALK, a receptor tyrosine kinase expressed specifically in the nervous system. Oncogene 1997, 14:439–449
10. Morris SW, Naeve C, Mathew P, James PL, Kirstein MN, Cui X, Witte DP: ALK, the chromosome 2 gene locus altered by the t(2;5) in non-Hodgkin's lymphoma, encodes a novel neural receptor tyrosine kinase that is highly related to leukocyte tyrosine kinase (LTK). Oncogene 1997, 14:2175–2188
11. Ben-Neriah Y, Bauskin AR: Leukocytes express a novel gene encoding a putative transmembrane protein-kinase devoid of an extracellular domain. Nature 1988, 333:672–676
12. Maru Y, Hirai H, Takaku F: Human ltk: gene structure and preferential expression in human leukemic cells. Oncogene Res 1990, 5:199–204
13. Bernards A, de la Monte SM: The ltk receptor tyrosine kinase is expressed in pre-B lymphocytes and cerebral neurons and uses a non-AUG translational initiator. EMBO J 1990, 9:2279–2287
14. Pulford K, Lamant L, Morris SW, Butler LH, Wood KM, Stroud D, Delsol G, Mason DY: Detection of anaplastic lymphoma kinase (ALK) and nucleolar protein nucleophosmin (NPM)-ALK proteins in normal and neoplastic cells with the monoclonal antibody ALK1. Blood 1997, 89:1394–1404
15. Shiota M, Fujimoto J, Takenaga M, Satoh H, Ichinohasama R, Abe M, Nakano M, Yamamoto T, Mori S: Diagnosis of t(2;5)(p23;q35)-associated Ki-1 lymphoma with immunohistochemistry. Blood 1994, 84:3648–3652
16. Duyster J, Bai RY, Morris SW: Translocations involving anaplastic lymphoma kinase (ALK). Oncogene 2001, 20:5623–5637
17. Stoica GE, Kuo A, Aigner A, Sunitha I, Souttou B, Malerczyk C, Caughey DJ, Wen D, Karavanov A, Riegel AT, Wellstein A: Identification of anaplastic lymphoma kinase as a receptor for the growth factor pleiotrophin. J Biol Chem 2001, 276:16772–16779
18. Stoica GE, Kuo A, Powers C, Bowden ET, Sale EB, Riegel AT, Wellstein A: Midkine binds to anaplastic lymphoma kinase (ALK) and acts as a growth factor for different cell types. J Biol Chem 2002, 277:35990–35998
19. Evans AE, D'Angio GJ, Randolph J: A proposed staging for children with neuroblastoma: children's cancer study group A. Cancer 1971, 27:374–378
20. Nakagawara A, Arima-Nakagawara M, Scavarda NJ, Azar CG, Cantor AB, Brodeur GM: Association between high levels of expression of the TRK gene and favorable outcome in human neuroblastoma. N Engl J Med 1993, 328:847–854
21. Nakagawara A, Azar CG, Scavarda NJ, Brodeur GM: Expression and function of TRK-B and BDNF in human neuroblastomas. Mol Cell Biol 1994, 14:759–767
22. Nakagawara A, Nakamura Y, Ikeda H, Hiwasa T, Kuida K, Sui MS, Zhao H, Cnaan A, Sakiyama S: High levels of expression and nuclear localization of interleukin-1 beta converting enzyme (ICE) and CPP32 in favorable human neuroblastomas. Cancer Res 1997, 57:4578–4584
23. Posmantur R, McGinnis K, Nadimpalli R, Gilbertsen RB, Wang K: Characterization of CPP32-like protease activity following apoptotic challenge in SH-SY5Y neuroblastoma cells. J Neurochem 1997, 68:2328–2337
24. Adida C, Berrebi D, Peuchmaur M, Reyes-Mugica M, Altieri DC: Anti-apoptosis gene, survivin, and prognosis of neuroblastoma. Lancet 1998, 351:882–883
25. Hiyama E, Hiyama K, Yokoyama T, Matsuura Y, Piatyszek MA, Shay JW: Correlating telomerase activity levels with human neuroblastoma outcomes. Nat Med 1995, 1:249–255
26. Lamant L, Pulford K, Bischof D, Morris SW, Mason DY, Delsol G, Mariame B: Expression of the ALK tyrosine kinase gene in neuroblastoma. Am J Pathol 2000, 156:1711–1721
27. Miyake I, Hakomori Y, Shinohara A, Gamou T, Saito M, Iwamatsu A, Sakai R: Activation of anaplastic lymphoma kinase is responsible for hyperphosphorylation of ShcC in neuroblastoma cell lines. Oncogene 2002, 21:5823–5834
28. Sakai R, Henderson JT, O'Bryan JP, Elia AJ, Saxton TM, Pawson T: The mammalian ShcB and ShcC phosphotyrosine docking proteins function in the maturation of sensory and sympathetic neurons. Neuron 2000, 28:819–833
29. Perucho M, Goldfarb M, Shimizu K, Lama C, Fogh J, Wigler M: Human-tumor-derived cell lines contain common and different transforming genes. Cell 1981, 27:467–476
30. Brodeur GM, Pritchard J, Berthold F, Carlsen NL, Castel V, Castelberry RP, De Bernardi B, Evans AE, Favrot M, Hedborg F, Kaneko M, Kemshead J, Lampert F, Lee RE, Look AT, Pearson AD, Philip T, Roald B, Sawada T, Seeger RC, Tsuchida Y, Voute PA: Revisions of the international criteria for neuroblastoma diagnosis, staging, and response to treatment. J Clin Oncol 1993, 11:1466–1477
31. Shimada H, Ambros IM, Dehner LP, Hata J, Joshi VV, Roald B, Stram DO, Gerbing RB, Lukens JN, Matthay KK, Castleberry RP: The International Neuroblastoma Pathology Classification (the Shimada system). Cancer 1999, 86:364–372
32. Ikeda I, Ishizaka Y, Tahira T, Suzuki T, Onda M, Sugimura T, Nagao M: Specific expression of the ret proto-oncogene in human neuroblastoma cell lines. Oncogene 1990, 5:1291–1296
33. Motegi A, Fujimoto J, Kotani M, Sakuraba H, Yamamoto T: ALK receptor tyrosine kinase promotes cell growth and neurite outgrowth. J Cell Sci 2004, 117:3319–3329
34. Slamon DJ, Clark GM, Wong SG, Levin WJ, Ullrich A, McGuire WL: Human breast cancer: correlation of relapse and survival with amplification of the HER-2/neu oncogene. Science 1987, 235:177–182
35. Tsuda H, Hirohashi S, Shimosato Y, Hirota T, Tsugane S, Yamamoto H, Miyajima N, Toyoshima K, Yamamoto T, Yokota J, Yoshida T, Sakamoto H, Terada M, Sugimura T: Correlation between long-term survival in breast cancer patients and amplification of two putative oncogene-coamplification units: hst-1/int-2 and c-erbB-2/ear-1. Cancer Res 1989, 49:3104–3108
36. Ganju P, O'Bryan JP, Der C, Winter J, James IF: Differential regulation of SHC proteins by nerve growth factor in sensory neurons and PC12 cells. Eur J Neurosci 1998, 10:1995–2008
37. Nakamura T, Komiya M, Gotoh N, Koizumi S, Shibuya M, Mori N: Discrimination between phosphotyrosine-mediated signaling properties of conventional and neuronal Shc adapter molecules. Oncogene 2002, 21:22–31
38. Nakamura T, Muraoka S, Sanokawa R, Mori N: N-Shc and Sck, two neuronally expressed Shc adapter homologs: their differential regional expression in the brain and roles in neurotrophin and Src signaling. J Biol Chem 1998, 273:6960–6967
39. O'Bryan JP, Songyang Z, Cantley L, Der CJ, Pawson T: A mammalian adaptor protein with conserved Src homology 2 and phosphotyrosine-binding domains is related to Shc and is specifically expressed in the brain. Proc Natl Acad Sci USA 1996, 93:2729–2734
40. Pelicci G, Troglio F, Bodini A, Melillo RM, Pettirossi V, Coda L, De Giuseppe A, Santoro M, Pelicci PG: The neuron-specific Rai (ShcC) adaptor protein inhibits apoptosis by coupling Ret to the phosphatidylinositol 3-kinase/Akt signaling pathway. Mol Cell Biol 2002, 22:7351–7363
41. Yuan J, Yankner BA: Apoptosis in the nervous system. Nature 2000, 407:802–809
42. De Vita G, Melillo RM, Carlomagno F, Visconti R, Castellone MD, Bellacosa A, Billaud M, Fusco A, Tsichlis PN, Santoro M: Tyrosine 1062 of RET-MEN2A mediates activation of Akt (protein kinase B) and mitogen-activated protein kinase pathways leading to PC12 cell survival. Cancer Res 2000, 60:3727–3731

LMO3 Interacts with Neuronal Transcription Factor, HEN2, and Acts as an Oncogene in Neuroblastoma

Mineyoshi Aoyama,[1] Toshinori Ozaki,[1] Hiroyuki Inuzuka,[1] Daihachiro Tomotsune,[3] Junko Hirato,[4] Yoshiaki Okamoto,[1] Hisashi Tokita,[2] Miki Ohira,[1] and Akira Nakagawara[1]

Divisions of [1]Biochemistry and [2]Animal Science, Chiba Cancer Center Research Institute; [3]Center for Functional Genomics, Hisamitsu Pharmaceutical Co., Inc., Chiba, Japan and [4]Department of Pathology, Gunma University School of Medicine, Gunma, Japan

Abstract

LIM-only proteins (LMO), which consist of LMO1, LMO2, LMO3, and LMO4, are involved in cell fate determination and differentiation during embryonic development. Accumulating evidence suggests that LMO1 and LMO2 act as oncogenic proteins in T-cell acute lymphoblastic leukemia, whereas LMO4 has recently been implicated in the genesis of breast cancer. However, little is known about the role of LMO3 in either tumorigenesis or development. In the present study, we have identified *LMO3* and *HEN2*, which encodes a neuronal basic helix-loop-helix protein, as genes whose expression levels were higher in unfavorable neuroblastomas compared with those of favorable tumors. Immunoprecipitation and immunostaining experiments showed that LMO3 was associated with HEN2 in mammalian cell nucleus. Human neuroblastoma SH-SY5Y cells stably overexpressing LMO3 showed a marked increase in cell growth, a promotion of colony formation in soft agar medium, and a rapid tumor growth in nude mice compared with the control transfectants. More importantly, the increased expression of LMO3 and HEN2 was significantly associated with a poor prognosis in 87 primary neuroblastomas. These results suggest that the deregulated expression of neuronal-specific LMO3 and HEN2 contributes to the genesis and progression of human neuroblastoma in a lineage-specific manner. (Cancer Res 2005; 65(11): 4587-97)

Introduction

The LIM domain–containing proteins are important regulators in determining cell fate and controlling cell growth and differentiation during embryonic development (1). The LIM domain is a highly conserved cysteine-rich zinc finger–like motif found in a variety of nuclear and cytoplasmic proteins and acts as a docking site for the assembly of multiprotein complexes (2–4). However, the precise role of the LIM domain is still unclear. Several distinct subgroups of the LIM domain–containing proteins are defined and some of them also possess a functionally divergent domain, including a DNA-binding homeodomain or a protein kinase domain (1, 2).

The LIM-only proteins (LMO) are one of the families of the LIM domain–containing proteins and possess only two tandem LIM domains. They consist of four members, including LMO1, LMO2, LMO3, and LMO4 (2, 4). *LMO1* and *LMO2* have been identified as the genes that are activated in human acute T-cell leukemia (T-cell ALL) by tumor-specific chromosomal translocations (4). Transgenic mice overexpressing LMO1 or LMO2 developed immature and aggressive T-cell leukemia, suggesting that these proteins act as T-cell oncoproteins (5–7). On the other hand, LMO4 has been identified as a nuclear protein that interacts with the adaptor protein Ldb1 (8). It has been shown recently that LMO4 is highly expressed in primary human breast cancers, and overexpression of LMO4 inhibits differentiation of mammary epithelial cells, suggesting that deregulated expression of LMO4 contributes to the breast carcinogenesis (9). LMO4 has also been reported to be associated with BRCA1 to repress its transcriptional activity (10). Thus, LMO1, LMO2, and LMO4 have been implicated in tumorigenesis. However, to date, little is known about the oncogenic function of LMO3, which has been discovered based on sequence homology with LMO1 (11).

The nuclear LMO proteins, which lack intrinsic DNA-binding activity, have been considered to be involved in transcriptional regulation (2), raising a possibility that they alter the transcription of target genes by forming a complex with other transcription factors with DNA-binding activity. Indeed, in T-cell acute lymphoblastic leukemia in children, a basic helix-loop-helix transcription factor, TAL1, is physically associated with LMO1 or LMO2 and enhances their oncogenic activities (12, 13). Interestingly, the neuronal-specific basic helix-loop-helix transcription factors, HEN1 and HEN2, were identified based on cross-hybridization with TAL1 (14, 15). Their expression was restricted to the developing nervous system and a human neuroblastoma cell line. However, the role of HEN1 and HEN2 in tumorigenesis has long been elusive.

Neuroblastoma is one of the most common childhood cancers and is originated from sympathoadrenal lineage of the neural crest (16). It is clinically and cytogenetically divided into two major subgroups with favorable and unfavorable prognosis (17). The recent molecular and cellular analyses have revealed that amplification of *MYCN* and *DDX1* as well as loss of heterozygosity at the region of chromosome 1p36 are strongly associated with a poor outcome, whereas high levels of expression of the neurotrophin receptors *TrkA*, *CD44*, and *Fyn*, are well correlated with favorable prognosis (16–23). However, we still do not know many other genes that play important roles in the genesis and progression of neuroblastoma. To identify the other genes closely involved in neuroblastoma, we have constructed several cDNA libraries from different subsets of neuroblastoma and randomly cloned 4,200 genes (24). Screening of the genes differentially expressed between favorable and unfavorable subsets of the tumor has identified *Nbla3267* as one of the genes expressed at higher levels in unfavorable than favorable neuroblastomas (25).

In the present study, we found that *Nbla3267* encoded the human LMO, LMO3, and that high expression of *LMO3* as well as *HEN2* was strongly associated with a poor prognosis of neuroblastoma. Furthermore, LMO3 interacted with HEN2 in mammalian

Requests for reprints: Akira Nakagawara, Division of Biochemistry, Chiba Cancer Center Research Institute, 666-2 Nitona, Chuoh-ku, Chiba 260-8717, Japan. Phone: 81-43-264-5431; Fax: 81-43-265-4459; E-mail: akiranak@chiba-cc.jp.

cell nucleus, and enforced expression of LMO3 in human neuroblastoma-derived cell line SH-SY5Y markedly enhanced tumor growth in nude mice, supporting the oncogenic role of LMO3 in neuroblastoma.

Materials and Methods

Patient population. The RNA samples obtained from 87 patients with neuroblastoma were subjected to semiquantitative and quantitative real-time reverse transcription-PCR (RT-PCR) analyses. All patients were diagnosed clinically as well as pathologically and tested for DNA ploidy, MYCN amplification, and TrkA expression. Tumors were staged according to the International Neuroblastoma Staging System criteria (26). Thirty-four patients were stage I, 14 were stage II, 8 were stage III, 26 were stage IV, and 5 were stage IVS. Stages I, II, and IVS were considered as favorable and stages III and IV as unfavorable. The patients were treated following the protocols proposed by the Japanese Infantile Neuroblastoma Cooperative Study (27) and the Study Group of Japan for Treatment of Advanced Neuroblastoma (28). The clinical follow-up ranged from 4 to 58 months, with a median of 36 months. We have a precise list of patient characteristics, including age, stage, and clinical follow-up time, and this list will be provided upon request.

Cloning of human *LMO3*, *HEN1*, and *HEN2*. To obtain a complete human *LMO3* cDNA, a cDNA library derived from human fetal brain (Stratagene, La Jolla, CA) was screened with a ^{32}P-labeled *Nbla3267* cDNA. Plaques showing positive signals were picked up and rescreened twice. To construct the expression plasmid for hemagglutinin (HA)–tagged LMO3-A, the cDNA fragment encoding the entire LMO3-A protein was amplified by PCR from the phage clone as a template using the primers designed to add a synthetic linker encoding the HA epitope on the NH_2-terminal side of LMO3-A (forward 5′-GGTACCATGGCTTACCCATACGATGTTCCAGATTACGCTAGCCTCTCAGTCCAGCCAGACAC-3′ and reverse 5′-TCAGATATCATTAGATCAGCGAACCTGGG-3′). The PCR product was digested with *Kpn*I and *Eco*RV and subcloned into the identical restriction sites of pcDNA3 expression plasmid to give pcDNA3-HA-LMO3-A. cDNA encoding human HEN1 (amino acid residues 1-133) or HEN2 (amino acid residues 1-135) was generated by reverse transcribing total RNA isolated from neuroblastoma cell line, IMR32, using a forward primer (5′-AAGGAATTCATGCTCAACTCAGACACCATG-3′) and a reverse primer (5′-ATAAGAATGCGGCCGCTCAGACGT-3′) for HEN1 and a forward primer (5′-AAGGAATTCATGCTGAGTCCGGACCAAGCA-3′) and a reverse primer (5′-ATAAGAATGCGGCCGCCTACACGTCCAGGACGTGGTT-3′) for HEN2. The amplified PCR products were digested with *Eco*RI and *Not*I and subcloned into the identical restriction sites of pcDNA3-FLAG expression plasmid to give pcDNA-FLAG-HEN1 and pcDNA3-FLAG-HEN2.

Generation of a polyclonal anti-LMO3 antibody. The polyclonal anti-LMO3 and anti-HEN2 antibodies were raised against a peptide "Cys" plus containing the amino acid sequence between positions 127 and 145 of LMO3 and the amino acid sequence between positions 1 and 19 of HEN2, respectively. The peptides and the polyclonal antibodies were produced by Biologica Co. (Nagoya, Japan).

Cell culture and transfection. Human neuroblastoma (SK-N-AS, SH-SY5Y, NB69, OAN, SK-N-BE, NGP, NLF, IMR32, NB1, and KP-N-NS), ALL (RPMI, KOPT, HSB, and MOLT), osteosarcoma (OST, SAOS-2, and U2OS), rhabdomyosarcoma (RMS-MK), colon cancer (COLO-320), breast cancer (MCF-7 and MDA-MB-453), melanoma (G361, G32TG, and A875), thyroid cancer (TTC11), small cell lung carcinoma (H1299), and cervical cancer (HeLa) cell lines and COS7 cells were maintained in RPMI 1640 or DMEM supplemented with 10% heat-inactivated fetal bovine serum (FBS), 100 IU/mL penicillin, and 100 μg/mL streptomycin at 37°C in an atmosphere of 5% CO_2 in the air. For transient transfection, COS7 cells were transfected with the indicated expression plasmids using FuGene 6 transfection reagent as recommended by the manufacturer (Roche Molecular Biochemicals, Mannheim, Germany). Stable transfections of SH-SY5Y cells were done with the empty plasmid (pcDNA3, Invitrogen, Carlsbad, CA) or with the expression plasmid for FLAG-tagged LMO3-A using Lipofect-AMINE Plus transfection reagent according to the manufacturer's instructions (Invitrogen). The transfected cells were cultured in the presence of G418 at a final concentration of 400 μg/mL (Sigma Chemical Co., St. Louis, MO). Thereafter, the selection medium was replaced every 3 days. Three weeks after the selection in G418, drug-resistant clones were isolated and allowed to proliferate in medium containing G418.

Reverse transcription-PCR analysis. Total RNA was prepared from cultured cells and human tissues by using Trizol reagent (Life Technologies, Grand Island, NY) or the RNeasy Mini kit (Qiagen, Valencia, CA). Reverse transcription was carried out using random primers and SuperScript II (Invitrogen). Following the reverse transcription, the resultant cDNA was subjected to PCR-based amplification. Oligonucleotides used to amplify *LMO3-A*, *LMO3-B*, *LMO1*, *LMO2*, *LMO4*, *Ldb1*, *Ldb2*, *TAL1*, *HEN1*, *HEN2*, and glyceraldehyde-3-phosphate dehydrogenase (*GAPDH*) mRNAs were as follows: *LMO3-A*: forward 5′-ACTGTGCTTACTGAACGGCCTC-3′ and reverse 5′-CCGGTCCTTGATCTTTCGGTTG-3′; *LMO3-B*: forward 5′-TGCAACTCAGACACGCCTAAG-3′ and reverse 5′-CCGGTCCTTGATCTTTCGGTTG-3′; *LMO1*: forward 5′-GCTCCACCCTCTACACCAAG-3′ and reverse 5′-CTGCCCTTCCTCATAGTCCA-3′; *LMO2*: forward 5′-AATGCGGGTGAAAGACAAAG-3′ and reverse 5′-CCCCAAAGTGCCTAAGAGTG-3′; *LMO4*: forward 5′-GCAAGGCAATGTGTATCATCT-3′ and reverse 5′-GCATTCTGCATTACTCTGACC-3′; *Ldb1*: forward 5′-CCAGGGAGCAGAAGACAGAA-3′ and reverse 5′-AGAGGCCCAGGTTCCAAG-3′; *Ldb2*: forward 5′-TAGCCCAAGTGCTGAAACAA-3′ and reverse 5′-TAAACTGCCCACAAAACCAA-3′; *TAL1*: forward 5′-GTTCTTAGGCTGCTGGGATG-3′ and reverse 5′-GATTTGGGACTGAGGGAAGA-3′; *HEN1*: forward 5′-AGAGACTGAGTCGGGCTTCA-3′ and reverse 5′-CAGGCGCAGAATCTCAATCT-3′; *HEN2*: forward 5′-CCCCAAGGGTTGTGGTTTTA-3′ and reverse 5′-TCTGAACTTCTGCCCTCATTCTTT-3′; and *GAPDH*: forward 5′-ACCTGACCTGCCGTCTAGAA-3′ and reverse 5′-TCCACCACCCTGTTGCTGTA-3′. Amplified products were electrophoretically separated on agarose gels and visualized by ethidium bromide staining. The gels were photographed under UV illumination.

Northern analysis. A human MTN blot (Clontech, Palo Alto, CA), a nylon membrane on which poly(A)$^+$ RNAs extracted from various human normal tissues were blotted, was used for analysis of the distribution of *LMO3* expression in human normal tissues. ^{32}P-labeled probe was prepared by random priming of the 2.5-kb restriction fragment of *LMO3* cDNA. The membrane was hybridized overnight at 65C in a solution containing 7.5% dextran sulfate, 1 mol/L NaCl, 1% *N*-lauroyl sarcosine, 100 μg/mL heat-denatured salmon sperm DNA, and the radiolabeled probe. The membrane was washed twice in 0.5 × SSC/0.1% *N*-lauroyl sarcosine at 50°C. Specific signals were obtained by autoradiography.

Section *in situ* hybridization. Section *in situ* hybridization was done as described previously (29). A riboprobe was synthesized with digoxygenin-UTP and T3 or T7 polymerase (Roche Molecular Biochemicals). The alkaline phosphatase reaction was done with nitroblue tetrazolium/5-bromo-4-chloro-3-indolyl phosphate (Roche Molecular Biochemicals). The riboprobe used for the section *in situ* hybridization were transcripts of the human cDNA fragments of the *LMO3* gene.

Immunohistochemistry. Neuroblastoma tissues were stained with immunoperoxidase method using anti-HEN2 antibody. They included unfavorable neuroblastomas with *MYCN* gene amplification and favorable neuroblastomas with a single copy of *MYCN* gene. Neuroblastoma specimens were fixed in 10% buffered formalin and embedded in paraffin, and 3 μm sections were applied to the immunostaining. Before incubation with anti-HEN2 antibody, the sections were treated with 0.05% Pronase in 0.05 mol/L Tris-HCl (pH 7.6) for 5 minutes. The sections were incubated with anti-HEN2 antibody, which was diluted to 1:200 at 4°C overnight. The biotin-streptavidin method (Nichirei, Tokyo, Japan) was done, and the sections were visualized with diaminobenzidine solution. The nuclei were counterstained with hematoxylin.

Immunofluorescent staining. COS7 cells were doubly transfected with the expression plasmids for HA-LMO3-A and FLAG-HEN2. Forty-eight hours after transfection, cells were fixed for 30 minutes with 3.7% formaldehyde in PBS and permeabilized with 0.2% Triton X-100 for 5 minutes, and nonspecific epitopes were blocked for 1 hour in PBS containing 3% bovine serum albumin. The cells were then incubated with a polyclonal anti-HA antibody (1:200 dilution, Medical and Biological Laboratories, Nagoya,

Japan) and a monoclonal anti-FLAG antibody (1:50, M2, Sigma Chemical). After three washes with PBS, cells were stained with a FITC- or a rhodamine-conjugated secondary antibody (1:200, Invitrogen). The coverslips were mounted onto glass slides, and the stained cells were viewed using a confocal laser scanning microscope (Olympus, Tokyo, Japan).

Western blot analysis and immunoprecipitation. After transfection, cells were rinsed twice with ice-cold PBS and then lysed immediately with SDS sample buffer. Equal amounts of proteins were separated under denaturing conditions by electrophoresis in 15% polyacrylamide gel containing SDS-PAGE and electrotransferred to polyvinylidene difluoride membrane (Immobilon-P, Millipore, Bedford, MA). After blocking in a solution containing 5% skim milk, the membrane was incubated with a monoclonal anti-FLAG, a polyclonal anti-HA, a polyclonal anti-LMO3, or a polyclonal anti-actin antibody (20-33, Sigma Chemical) and then incubated with a horseradish peroxidase–conjugated goat anti-mouse or anti-rabbit secondary antibody (Jackson ImmunoResearch Laboratories, West Grove, PA). Protein bands were visualized with an enhanced chemiluminescence (Amersham Pharmacia Biotech, Piscataway, NJ). For immunoprecipitation, transfected cells were lysed in EBC buffer [50 mmol/L Tris-HCl (pH 7.5), 120 mmol/L NaCl, 0.5% NP40, 1 mmol/L phenylmethylsulfonyl fluoride] containing protease inhibitor mixture (Sigma Chemical). The precleared soluble supernatants were mixed with a polyclonal anti-HA or a monoclonal anti-FLAG antibody and incubated for 2 hours at 4°C. Protein A-Sepharose beads were then added to the reaction mixtures and incubated for 1 hour at 4°C. The immune complexes were washed with the lysis buffer thrice at 4°C. The bound proteins were resuspended in SDS sample buffer, resolved by SDS-PAGE, and analyzed by Western blotting.

Cell proliferation and soft agar assay. Cells were seeded in triplicate in 24-well plates (5×10^3 per well) in culture medium containing 10% or 1% FBS. Cells were allowed to adhere to the bottom of the cell culture dish for 24 hours. At the indicated times, cells were trypsinized and cell counting was carried out using a Coulter Counter (Coulter Electronics Ltd., Hialeah, Finland). For soft agar assay, 2.5×10^3 cells of the stable transfectants or the parental SH-SY5Y cells were seeded in triplicate in 35-mm cell culture plates containing 0.2% agar and RPMI 1640 supplemented with 10% FBS. After 21 days, colonies with diameters >300 μm were scored as positive.

Tumor formation in nude mice. For tumor formation, 6-week-old female athymic *nu/nu* mice (Charles River Laboratory, Sulzfeld, Germany) were injected into the femur with 5×10^6 parental SH-SY5Y cells or SH-SY5Y cells transfected with the empty plasmid or with the expression plasmid encoding LMO3-A suspended in 100 μL PBS. Tumor size and body weight were measured once weekly and mice were sacrificed 7 weeks after injection. For histologic examinations, tumor tissues were fixed in fresh 10% buffered formalin and embedded in paraffin. The handling of animals was in accordance with the guidelines of the Chiba Cancer Center Research Institute (Chiba, Japan).

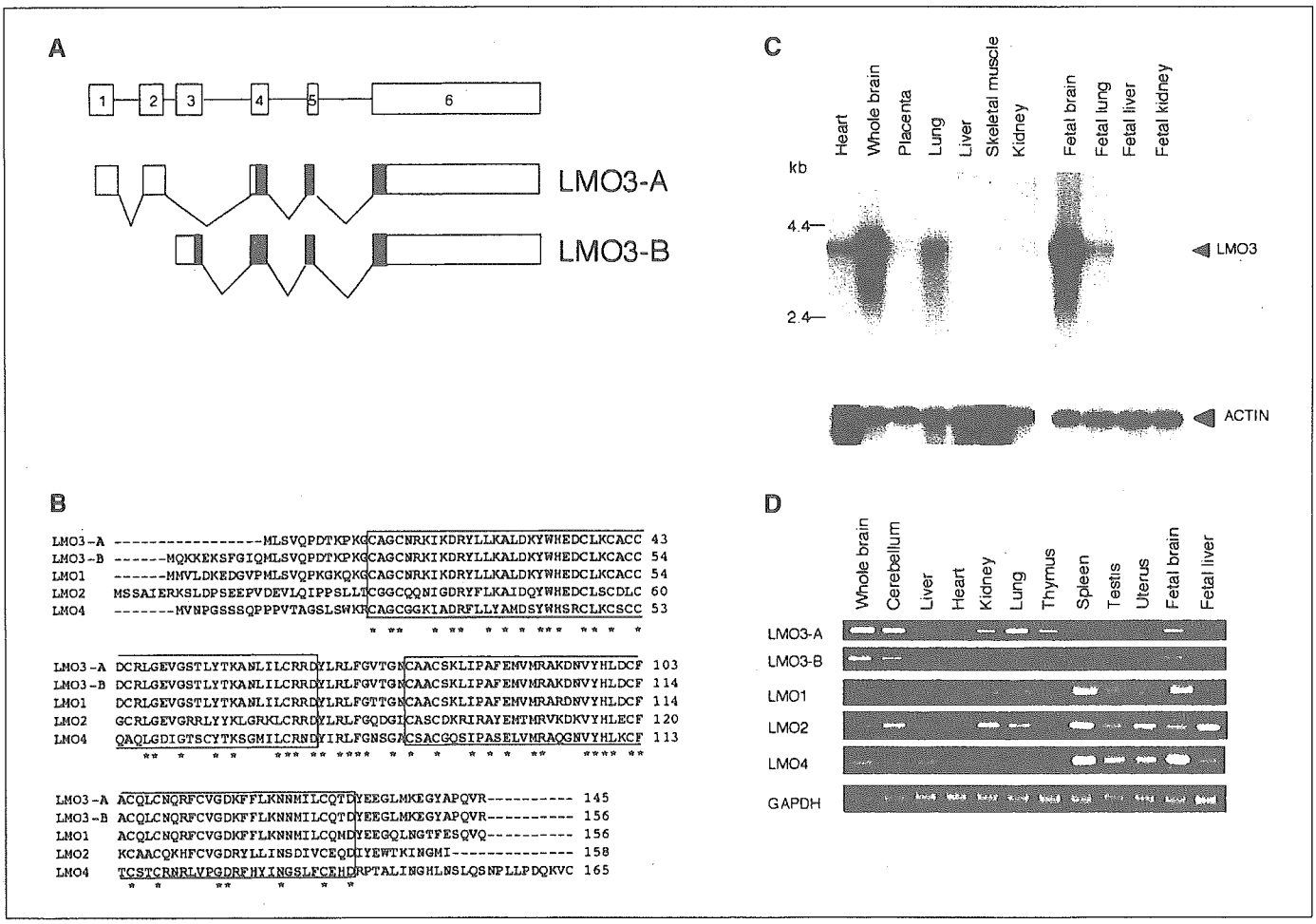

Figure 1. Identification of human LMO3-A and LMO3-B and their relation to the other LMO family members. *A*, schematic representation of the exons of human *LMO3* gene. *Solid* and *open boxes*, coding and untranslated regions, respectively. *B*, deduced amino acid sequences of human LMO3-A and LMO3-B and their alignments with those of human LMO1, LMO2, and LMO4. *Asterisks*, identical amino acid residues. Two LIM domains are *boxed*. *C*, tissue-specific expression of *LMO3*. Human multiple tissue Northern blots containing poly(A)$^+$ RNA were hybridized with a radiolabeled human *LMO3* cDNA (*top*) or with a radioactive probe derived from human *β-actin* cDNA (*bottom*). β-actin was used as a control for equal loading. The 2-kb band was hybridized ubiquitously, and an additional 1.8-kb band was hybridized in heart and skeletal muscle with the β-actin probe. *D*, coordinated expression of *LMO3-A* and *LMO3-B* in various human tissues. Total RNA isolated from the indicated human tissues was subjected to RT-PCR analysis to examine the expression levels of *LMO3-A*, *LMO3-B*, *LMO1*, *LMO2*, and *LMO4*. *GAPDH* expression is shown as an internal control.

Quantitative real-time PCR. Total RNA prepared from primary neuroblastomas was reverse transcribed into cDNA (SuperScript II kit) and subjected to the real-time PCR. The expression level of *GAPDH* was measured in all samples to normalize *LMO3* and *HEN2* expression according to the manufacturer's instructions (Applied Biosystems, Foster City, CA). Oligonucleotide primers and TaqMan probes, which were labeled at the 5′ end with the reporter dye 6-carboxyfluorescein (FAM) and at the 3′ end with the quencher dye 6-carboxytetramethylrhodamine (TAMRA), were as follows: *LMO3*: forward 5′-TCTGAGGCTCTT-TGGTGTAACG-3′, reverse 5′-CCAGGTGGTAAACATTGTCCTTG-3′, and probe 5′-FAM-AAACTGCGCTGCCTGTAGTAAGCTCATCC-TAMRA-3′ and *HEN2*: forward 5′-CCCCAAGGGTTGTGGTTTTA-3′, reverse 5′-TCTGAACTTCTGCCCTCATTCTTT-3′, and probe 5′-FAM-TTGAGTTCTCC-TACATTCATCCGCCACAA-TAMRA-3′. Amplification and detection were done using the ABI Prism 7700 Sequence Detection System (Applied Biosystems).

Statistical analysis. Student's *t* tests were used to explore possible associations between *LMO3* expression and other factors. Because the values of the *LMO3* expression were skewed, a log transformation was used to achieve the normality in the analyses using *t* test and Cox regression. The distinction between high and low levels of *LMO3* expression was based on the median value (low, *LMO3* < 0.2493 e.u.; high, *LMO3* > 0.2493 e.u.) regardless of tumor stage, *MYCN* copy number, or survival. The distinction between high and low levels of *HEN2* expression was based on the distribution of the values (low, undetectable; high, detectable). χ^2 tests were used to examine possible associations between *HEN2* expression and other factors, such as tumor stage. Kaplan-Meier survival curves were calculated, and survival distributions were compared using the log-rank test. Cox regression models were used to explore associations among *LMO3* expression, *HEN2* expression, age, *MYCN* amplification, mass screening, origin, and survival. Statistical significance was declared if $P < 0.05$. The statistical analysis was done using Stata Statistical Software Release 7.0 (Stata Corp., College Station, TX, 2001).

Results

Identification of the human *LMO3* gene. To identify the genes specifically involved in the genesis and progression of neuroblastoma, we have previously constructed cDNA libraries from the primary neuroblastomas and screened for the differentially expressed genes between the tumors with good and poor clinical outcome (25). One of the cDNA clones, *Nbla3267*, significantly overexpressed in the poor prognostic neuroblastomas contained a partial nucleotide sequence encoding a LMO family protein, LMO3. To obtain the missing 5′ part of the *LMO3* cDNA, we screened a cDNA library derived from human fetal brain. From ~6 × 10^5 recombinant phage clones, 10 independent phage clones were isolated. Sequence analysis

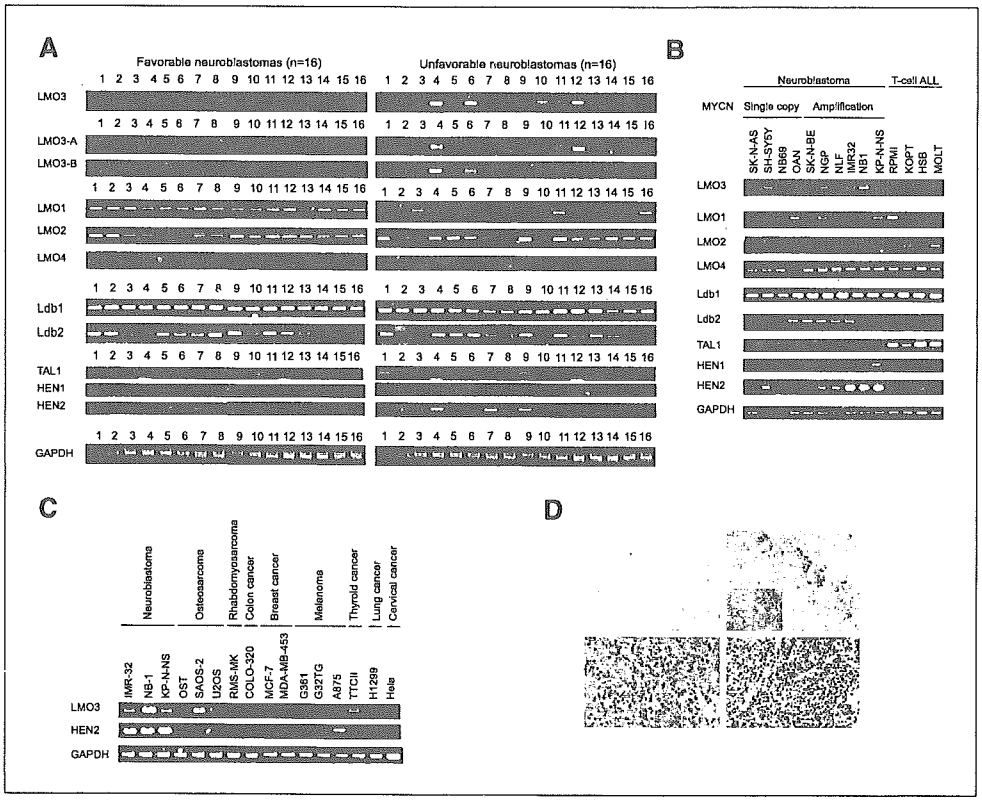

Figure 2. Increased expression of *LMO3* and *HEN2* in unfavorable neuroblastomas and neuroblastoma-derived cell lines. *A*, expression of *LMO3* and *LMO*-related genes in primary neuroblastomas with favorable (stage I, a single copy of *MYCN* and high expression of *TrkA*) and unfavorable (stages III and IV, *MYCN* amplification and decreased expression of *TrkA*) characteristics. Total RNA was isolated from the indicated neuroblastoma tissues, reverse transcribed, and amplified by PCR to examine the expression levels of *LMO3*, *LMO3-A*, *LMO3-B*, *LMO1*, *LMO2*, *LMO4*, *Ldb1*, *Ldb2*, *TAL1*, *HEN1*, and *HEN2*. Expression of *GAPDH* serves as an internal control. PCR products were visualized by ethidium bromide staining. *B*, expression of *LMO3* and *LMO*-related genes in neuroblastoma cell lines without *MYCN* amplification (SK-N-AS, SH-SY5Y, NB69, and OAN), neuroblastoma cell lines with *MYCN* amplification (SK-N-BE, NGP, NLF, IMR32, NB1, and KP-N-NS), and ALL cell lines (RPMI, KOPT, HSB, and MOLT). Total RNA prepared from the indicated cultured cells was subjected to RT-PCR analysis. Expression of *GAPDH* serves as an internal control. *C*, expression of *LMO3* and *HEN2* in various tumor-derived cell lines. Total RNA prepared from the indicated culture cells was subjected to RT-PCR analysis as described above. *D*, section *in situ* hybridization of neuroblastoma with the *LMO3* probe. Serial sections of the favorable neuroblastoma tissue (*top left* and *inset*) or the unfavorable one with *MYCN* amplification (*top right* and *inset*) were prepared, and expression of the *LMO3* gene was examined by section *in situ* hybridization. The *LMO3* transcripts are positive in unfavorable neuroblastoma. Immunohistochemical staining of HEN2 in primary neuroblastoma tissues. HEN2 is strongly positive in the nucleus of most tumor cells with *MYCN* amplification (*bottom right*), whereas it is negative in the favorable neuroblastoma tissue (*bottom left*).

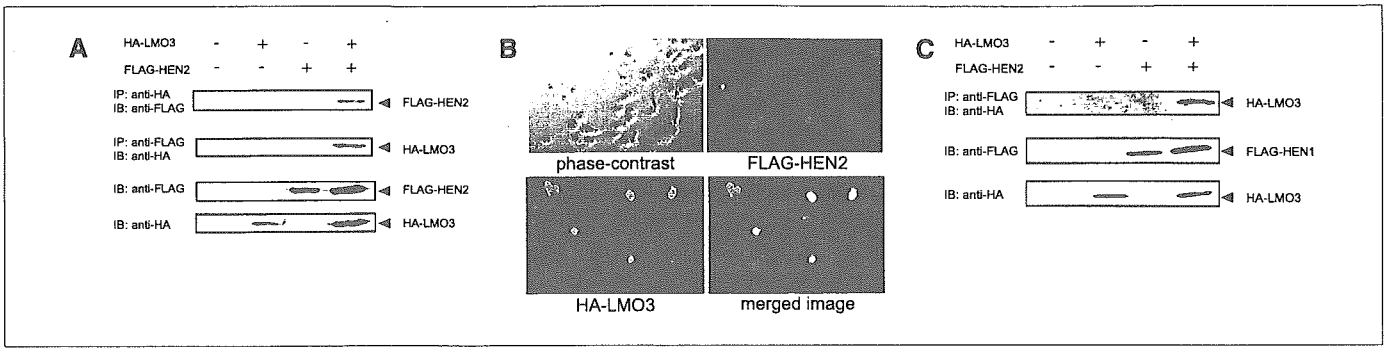

Figure 3. LMO3 interacts with HEN2 in mammalian cells. *A*, coimmunoprecipitation analysis. COS7 cells were transfected with the indicated expression plasmids. Forty-eight hours after transfection, whole cell lysates were prepared and subjected to the immunoprecipitation/Western analysis (*top* and *top middle*). Whole cell lysates were monitored on immunoblot for the expression of FLAG-HEN2 (*bottom middle*) and HA-LMO3-A (*bottom*). *B*, nuclear colocalization of LMO3 and HEN2 in cultured cells. COS7 cells were cotransfected with the expression plasmids for HA-LMO3-A and FLAG-HEN2. Forty-eight hours after transfection, cells were fixed and incubated with the polyclonal anti-HA and monoclonal anti-FLAG antibodies. Cells were then processed for double immunofluorescence using the FITC-conjugated anti-rabbit IgG (*green*) and with the rhodamine-conjugated anti-mouse IgG (*red*). The merged images (*yellow*) suggest the nuclear colocalization of LMO3 and HEN2. The phase-contrast images are also shown. *C*, coimmunoprecipitation of FLAG-HEN1 and HA-LMO3. Whole cell lysates prepared from COS7 cells transfected with the indicated combinations of the expression plasmids were immunoprecipitated with the anti-FLAG antibody followed by immunoblotting with the anti-HA antibody (*top*). Levels of FLAG-HEN1 and HA-LMO3 were also examined by immunoblotting with the anti-FLAG antibody (*middle*) and with the anti-HA antibody (*bottom*), respectively.

revealed that they were divided into two types, designated LMO3-A (145 amino acids) and LMO3-B (156 amino acids), with the different translation initiation sites. The NH_2-terminal region of LMO3-A was identical to that of the previously reported LMO3 protein (11). As shown in Fig. 1*A*, the putative translation initiation sites of LMO3-A and LMO3-B were located within exons 4 and 3, respectively. Because *LMO3* is a single gene, it is likely that LMO3-A and LMO3-B arise from differential splicing

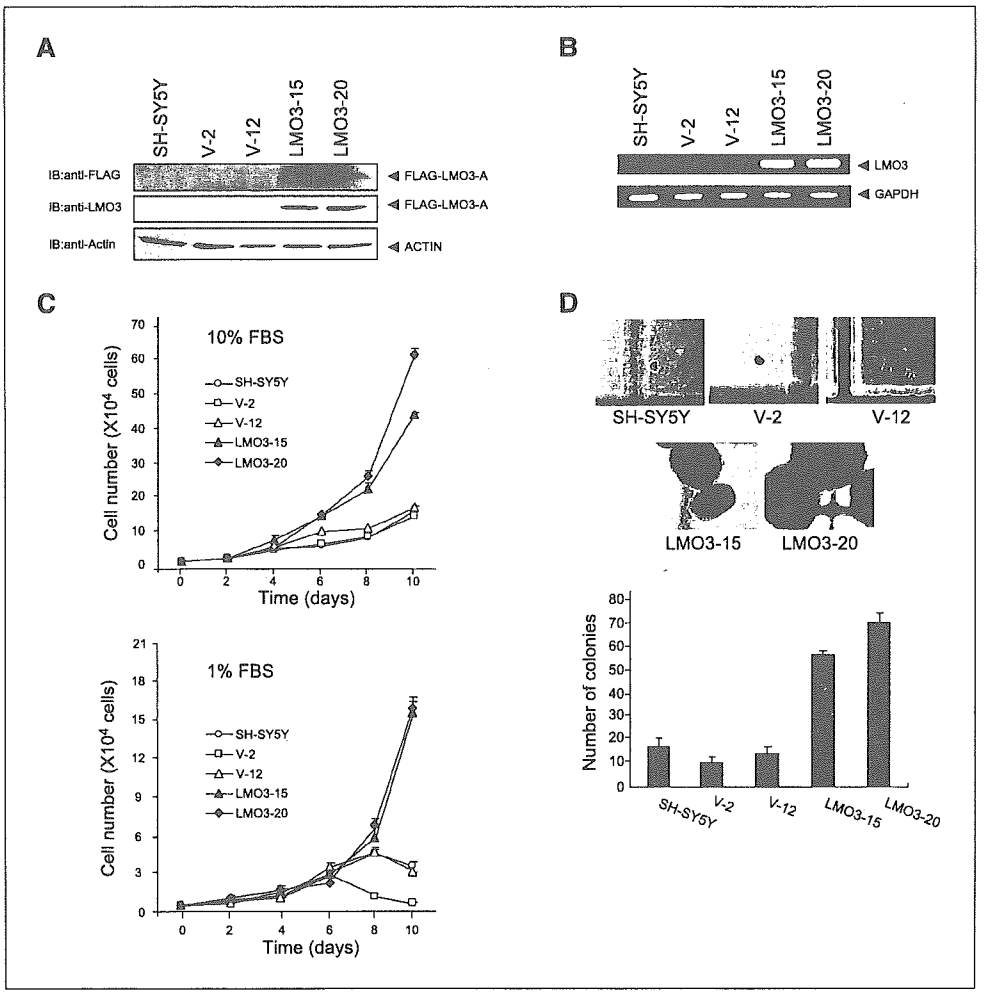

Figure 4. Growth-promoting activity of LMO3 in SH-SY5Y cells. *A*, stable SH-SY5Y transfectants expressing exogenous FLAG-LMO3-A. SH-SY5Y cells were stably transfected with the empty plasmid or with the expression plasmid for FLAG-LMO3-A and maintained in the presence of G418 (at a final concentration of 400 μg/mL) for 3 weeks. Whole cell lysates prepared from the indicated drug-resistant cell clones in addition to the parental SH-SY5Y cells were subjected to Western blot analysis using the anti-FLAG (*top*), anti-LMO3 (*middle*), or anti-actin (*bottom*) antibody. *B*, RT-PCR analysis of LMO3 in the indicated stable transfectants along with the parental SH-SY5Y cells. Expression of GAPDH serves as an internal control. *C*, effects of LMO3 overexpression on cell growth in SH-SY5Y cells. SH-SY5Y cells and the indicated transfectants were grown in the culture medium containing 10% (*top*) or 1% (*bottom*) FBS. Cells were harvested at 48-hour time intervals and number of cells was counted in triplicate. *Points*, means from three independent experiments; *bars*, SE. *D*, anchorage-independent growth of LMO3-overexpressing transfectants. The parental SH-SY5Y cells and the indicated transfectants (2.5×10^3 cells per dish) were grown in soft agar medium. After 3 weeks of culture, cells were examined by phase-contrast microscopy (*top*), and the numbers of colonies with a diameter of >300 μm were counted (*bottom*). *Columns*, means from three independent experiments; *bars*, SE.

or alternative promoter usage. Amino acid sequence alignment of LMO3 with the other LMO family proteins (LMO1, LMO2, and LMO4) showed a significant homology among them (Fig. 1*B*). LIM domains of LMO3 presented 98%, 60%, and 55% amino acid homology with those of LMO1, LMO2, and LMO4, respectively.

To determine the expression pattern of human *LMO3* mRNA, we did Northern blot analysis on a human multiple tissues blot using -actin as a control. As shown in Fig. 1*C*, *LMO3* mRNA (~4 kb) was abundantly expressed in brain and at relatively low levels in the heart and lung but not in the other tissues examined. Similar to the adult tissues, *LMO3* mRNA was expressed predominantly in fetal brain, with a lower level in fetal lung. We then compared the tissue distribution of *LMO3-A* expression with those of *LMO3-B* and the other *LMO* family gene expression in various human adult and fetal tissues by RT-PCR (Fig. 1*D*). The expression pattern of *LMO3-A* was similar to that of *LMO3-B*, with relatively higher levels in brain, cerebellum, and fetal brain. In contrast, *LMO2* and *LMO4* were expressed ubiquitously in human tissues, and *LMO1* was expressed at higher levels in spleen and fetal brain.

Expression of *LMO3* and *HEN2* in aggressive neuroblastomas. As described previously, LMO family protein interacts with the nuclear LIM domain–binding protein 1 and 2 (Ldb1 and Ldb2), which act as adaptors for several LIM domain–containing proteins (30–32), and also binds to the basic helix-loop-helix transcription factor, TAL1, to regulate its transcriptional activity (12, 33, 34). Of interest, HEN1 and HEN2 were previously identified based on their homology with TAL1, and it was shown that LMO3 was associated with HEN1 (35). Furthermore, TAL1 was coexpressed with LMO1 or LMO2 in T-cell ALL (36), and double transgenic mice overexpressing TAL1 and LMO1 or LMO2 developed leukemia (37). As shown in Fig. 2*A*, *LMO3* (A and B) and *HEN2* were expressed at higher levels in unfavorable neuroblastomas compared with favorable tumors, whereas the levels of *LMO1* expression were predominantly high in the favorable tumors. No significant changes in the expression levels of *LMO2*, *Ldb1*, and *Ldb2* were detected between unfavorable and favorable neuroblastomas. *LMO4*, *TAL1*, and *HEN1* showed extremely low levels of expression in both types of neuroblastoma. We then studied the expression of these genes in 10 neuroblastoma and 4 T-cell ALL cell lines to examine the presence or absence of the lineage specificity, neuronal or hematopoietic. Consistent with the previous reports (36), *LMO2* and *TAL1* were coexpressed in T-cell ALL-derived cell lines (RPMI, KOPT, HSB, and MOLT; Fig. 2*B*). However, of interest, *LMO3* and *Ldb2* were expressed predominantly in neuroblastoma cell lines compared with the leukemia-derived lines. In addition, *HEN2* tended to be less highly expressed in leukemia cells compared with neuroblastoma cells. *HEN1* expression was also restricted to neuroblastoma but limited to only a few cell lines. On the other hand, there was no difference in the expression of *LMO4* and *Ldb1* between neuroblastoma-derived and T-cell ALL-derived cell lines. Interestingly, coexpression of *LMO3* and *HEN2* was observed in the majority of neuroblastoma cell lines but not in the other tumor-derived cell lines with different origin (Fig. 2*C*). These results revealed that only *LMO3* and *HEN2* were expressed at high levels in aggressive neuroblastomas in a neuronal-specific pattern.

Figure 2*D* shows the results of *in situ* hybridization for *LMO3* in primary neuroblastomas. *LMO3* mRNA was expressed in a stage IV neuroblastoma with *MYCN* amplification, whereas it was negative in a stage I tumor with a single copy of *MYCN* and high expression of *TrkA*. Unfortunately, our antibody raised against human LMO3 protein did not work for the immunohistochemical analysis. The immunostaining of HEN2 was also strongly positive in the nuclei of most tumor cells in *MYCN*-amplified neuroblastoma, albeit it was negative in favorable subset of the tumor (Fig. 2*D*).

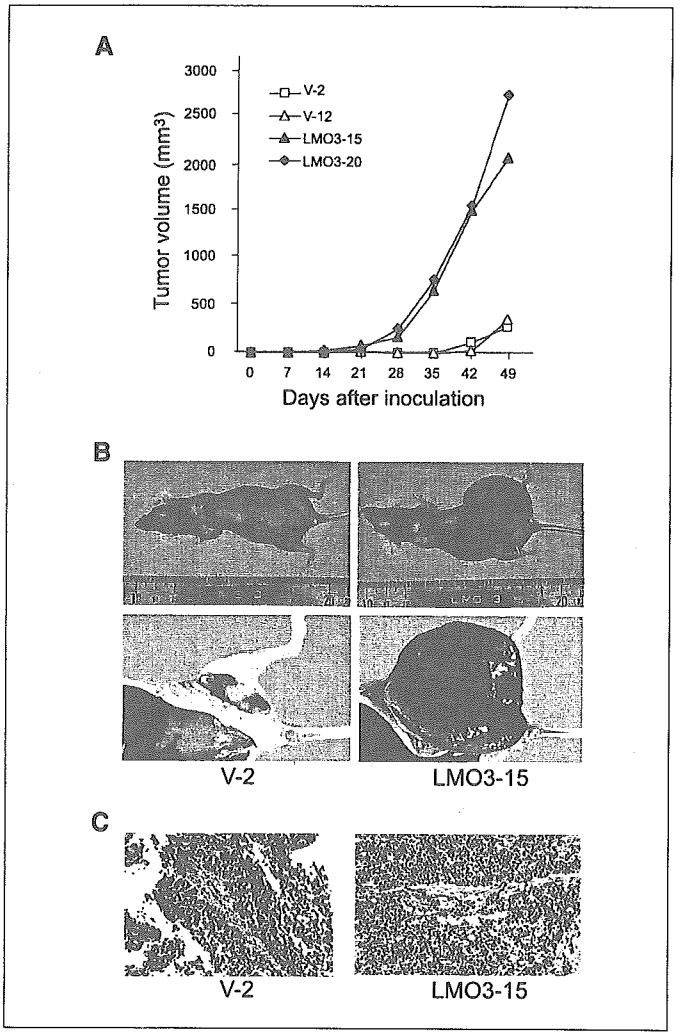

Figure 5. Tumor growth in nude mice. *A*, nude mice were injected s.c. with 5×10^6 of SH-SY5Y cells or the indicated stable transfectants and tumor volumes were estimated weekly. *Points*, mean of 8 to 11 independent tumors. *B*, photographs of the tumors 49 days after s.c. injection of V-2 (*left*) and LMO3-15 cells (*right*) into nude mice. *C*, paraffin sections of the tumors arising from V-2 (*left*) and LMO3-15 cells (*right*) were stained with H&E.

LMO3 physically interacts with HEN2. Because LMO3 and HEN2 were coexpressed in the majority of unfavorable neuroblastomas as well as neuroblastoma cell lines, we examined whether LMO3 could interact with HEN2 in mammalian cells. Whole cell lysates prepared from COS7 cells transfected with the expression plasmids for HA-tagged LMO3 and FLAG-tagged HEN2 were immunoprecipitated with the anti-HA or with the anti-FLAG antibody followed by immunoblotting with the anti-FLAG or with the anti-HA antibody, respectively. As shown in Fig. 3*A*, FLAG-HEN2 was coimmunoprecipitated with HA-LMO3. We then examined the subcellular distribution of LMO3 and

HEN2. COS7 cells were cotransfected with the expression plasmids for HA-LMO3 and FLAG-HEN2 and double stained with anti-HA and anti-FLAG antibodies. As shown in Fig. 3*B*, LMO3 as well as HEN2 appear exclusively nuclear. On closer inspection by merging two images, these two proteins colocalized in the nucleus. Consistent with the previous reports (35), HA-LMO3 was coimmunoprecipitated with FLAG-HEN1 under our experimental conditions (Fig. 3*C*).

Overexpression of LMO3 accelerates growth of SH-SY5Y neuroblastoma cells. We addressed the question whether LMO3 could induce cell growth of neuroblastoma. To this end, we transfected the expression plasmid for FLAG-LMO3-A or the empty plasmid into SH-SY5Y neuroblastoma cells and established two stable transfectants overexpressing FLAG-LMO3-A (named as LMO3-15 and LMO3-20). As shown in Fig. 4*A*, the expression levels of FLAG-LMO3-A were higher in LMO3-15 and LMO3-20 cells than in the parental SH-SY5Y and the control transfectants (V-2 and V-12). LMO3-15 expressed FLAG-LMO3-A at the level comparable with that in LMO3-20. Similar results were also obtained by RT-PCR analysis (Fig. 4*B*). No obvious morphologic changes could be observed in LMO3-15 and LMO3-20 cells (data not shown). As shown in Fig. 4*C*, LMO3-15 and LMO3-20 cells proliferated at a much faster rate than the control transfectants and SH-SY5Y cells in culture medium containing 10% serum. More importantly, LMO3-15 and LMO3-20 cells continued to grow exponentially even in the low serum culture medium, whereas the growth of the vector-transfected cells as well as SH-SY5Y cells was significantly suppressed under this condition.

To examine whether the LMO3-A-overexpressing cells have an ability to grow in soft agar medium, each transfectants were cultured in soft agar medium for 3 weeks. The numbers of colonies with diameters >300 μm formed by each transfectants in soft agar were scored. LMO3-15 and LMO3-20 cells formed large distinct colonies and showed a statistically significant increase in the number of colonies compared with the vector-transfected cells and SH-SY5Y cells (Fig. 4*D*). These results strongly suggest that overexpression of LMO3 is sufficient to induce malignant transformation in neuroblastoma cells. We also tried to obtain the cells stably transfected with HEN2 but never been successful with unknown reason.

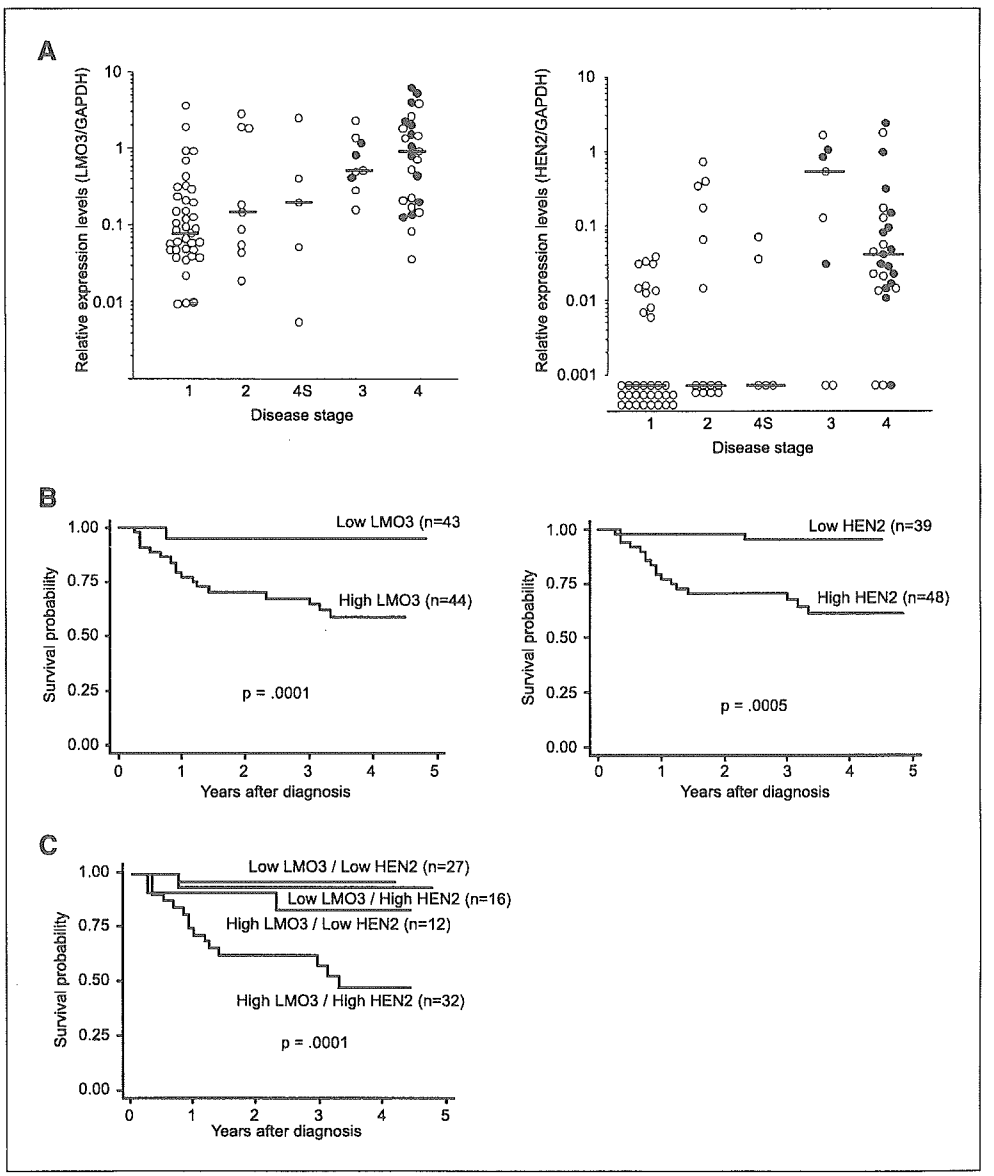

Figure 6. Expression of *LMO3* and *HEN2* mRNA in 87 primary neuroblastomas. *A*, expression levels of *LMO3* (*left*) and *HEN2* (*right*) transcripts in 87 primary neuroblastoma samples categorized by the patient's clinical stage were examined by a quantitative real-time RT-PCR. Relative expression levels of *LMO3* or *HEN2* mRNA were determined by calculating the ratio between *GAPDH* and *LMO3* or *HEN2*. *Bars*, median levels of *LMO3* or *HEN2* expression in each stage; *open* and *closed circles*, samples from patients who are alive and dead, respectively. *B* and *C*, Kaplan-Meier survival curves of patients with neuroblastomas based on high or low expression of *LMO3*, *HEN2* (*B*), or *LMO3* and *HEN2* (*C*).

LMO3 induces marked tumor growth in nude mice. SH-SY5Y cells with a single copy of *MYCN* form tumors in nude mice, although the growth rate is slow compared with that of the other neuroblastoma cell lines with *MYCN* amplification (38). To examine whether overexpression of LMO3 in SH-SY5Y cells could affect the tumor growth *in vivo*, we injected the each transfectants into the left flank of athymic nude mice, and the tumor volumes were measured weekly. V-2 and V-12 cells slowly formed tumors with similar kinetics and of similar sizes 35 to 42 days after injection (Fig. 5*A*). In contrast, the tumors grew rapidly in nude mice implanted with LMO3-15 or LMO3-20 cells. The sizes of the excised tumors from the LMO3-15-implanted mice on day 49 were >10-fold larger than those of control mice (Fig. 5*B*) and showed histologically undifferentiated neuroblastoma with small round cell shapes and small amounts of stromal components (Fig. 5*C*).

Expression of *LMO3* and *HEN2* is associated with a poor outcome of neuroblastoma. To verify whether a significant relationship could be observed between the expression of *LMO3* and/or *HEN2* in primary neuroblastomas and the patients' survival, we quantitatively measured the expression levels of *LMO3* and *HEN2* mRNA in 87 primary tumors by using a quantitative real-time RT-PCR. The values of the levels of *LMO3* and *HEN2* expression were normalized to that of *GAPDH* expression [relative expression values (REV)]. The high level of *LMO3* expression was significantly associated with high expression of *HEN2* (Student's *t* tests, mean ± SE: 1.43 ± 0.27 REV, n = 48 versus 0.54 ± 0.17 REV, n = 39; P = 0.001), older age (≥1-year-old: 1.37 ± 0.29, n = 32 versus <1-year-old: 0.84 ± 0.21, n = 55; P = 0.008), advanced disease stages (stages III + IV: 1.83 ± 0.35, n = 34 versus stages I + II + IVS: 0.52 ± 0.14; P < 0.00005; Fig. 6*A*), low levels of *TrkA* expression (low TrkA: 1.63 ± 0.34, n = 37 versus high *TrkA*: 0.59 ± 0.15, n = 50; P = 0.0003), *MYCN* amplification (amplification: 1.91 ± 0.44, n = 27 versus single copy: 0.64 ± 0.13, n = 60; P = 0.0002), and sporadic cases of neuroblastoma (sporadic: 1.68 ± 0.32, n = 39 versus mass screening: 0.51 ± 0.14, n = 48; P < 0.00005). The high level of *HEN2* expression was also significantly correlated with high expression of *LMO3* (χ^2 tests: P = 0.001), older age (P < 0.0005), advanced stages (P < 0.0005; Fig. 6*B*), low *TrkA* expression (P < 0.0005), *MYCN* amplification (P < 0.0005), and sporadic cases of neuroblastoma (P < 0.0005). Thus, high expression of *LMO3* and *HEN2* was well associated with conventional markers indicating the poor prognosis of neuroblastoma.

We next tested if expression levels of *LMO3* and *HEN2* could have prognostic significance in primary neuroblastomas. The results for log-rank tests showed that high expression of *LMO3* or *HEN2* was significantly associated with poor survival (P = 0.0002 and 0.0005, respectively; Fig. 6*C* and *D*). Remarkably, the combination of high expression of both *LMO3* and *HEN2* showed the significantly worse prognosis compared with the other combinations of *LMO3* and *HEN2* expression levels as shown in Fig. 6*E*. As expected, older patients and the patients with advanced tumors, low expression of *TrkA*, amplified *MYCN*, and the tumors found by mass screening were associated with short time to survival (P < 0.00005). However, the adrenal origin of the tumor was not associated with the outcome (P = 0.19; data not shown).

The univariate analysis suggested that *LMO3* expression (P < 0.0005), *HEN2* expression (P = 0.004), age (P < 0.0005), *MYCN* amplification (P < 0.0005), and mass screening (P = 0.001) were of prognostic importance, supporting the results of the log-rank test (Table 1). Furthermore, the multivariate analysis showed that

Table 1. Simple Cox regression models using LMO3 expression and dichotomous factors of HEN2 expression, age, MYCN amplification, mass screening, and origin (n = 87)

Model	Factor	P	Hazard ratio (95% confidence interval)
A	LMO3 expression (high vs low)	<0.0005	1.80 (1.32-2.47)
B	HEN2 expression (high vs low)	0.004	8.69 (2.00-37.7)
C	Age (≥1 vs <1 y)	<0.0005	8.75 (2.87-26.7)
D	MYCN amplification (1 copy vs >1 copy)	<0.0005	0.049 (0.014-0.171)
E	Mass screening (+ vs −)	0.001	0.032 (0.004-0.237)
F	Origin (adrenal gland vs others)	0.20	2.06 (0.684-6.23)

NOTE: All variables with two categories, except *LMO3* expression (log). Hazard ratio shows the relative risk of death of first category relative to the second. Because all patients with advanced tumor stages and low expression of *TrkA* had died of the tumor, a Cox regression model with the tumor stage or *TrkA* expression was not fitted.

Table 2. Multiple Cox regression models using LMO3 expression and dichotomous factors of HEN2 expression, age, MYCN amplification, mass screening, and origin (n = 87)

Model	Factor	P	Hazard ratio (95% confidence interval)
A	LMO3 expression (high vs low)	0.005	1.61 (1.16-2.23)
	HEN2 expression (high vs low)	0.029	5.32 (1.19-23.9)
B	LMO3 expression (high vs low)	0.005	1.62 (1.15-2.28)
	Age (>1 vs <1 y)	0.002	5.79 (1.86-18.1)
C	LMO3 expression (high vs low)	0.066	1.36 (0.98-1.89)
	MYCN amplification (1 copy vs >1 copy)	<0.0005	0.075 (.02-.282)
D	LMO3 expression (high vs low)	0.044	1.42 (1.01-2.01)
	Mass screening (+ vs −)	0.005	0.051 (0.007-0.404)
E	LMO3 expression (high vs low)	<0.0005	1.78 (1.31-2.41)
	Origin (adrenal gland vs others)	0.21	2.02 (0.666-6.12)

NOTE: All variables with two categories, except *LMO3* expression (log). Hazard ratio shows the relative risk of death of first category relative to the second.

LMO3 expression was significantly associated with survival after controlling *HEN2* expression ($P = 0.005$), age ($P = 0.005$), mass screening ($P = 0.044$), and origin ($P < 0.0005$), suggesting that *LMO3* expression was an independent prognostic factor from the other factors (Table 2). *LMO3* expression was marginally associated with survival after controlling *MYCN* amplification ($P = 0.066$). On the other hand, because *HEN2* expression was highly associated with age, *MYCN* amplification, and mass screening, it was not significantly associated with survival after controlling age, *MYCN* amplification, and mass screening in the corresponding multiple Cox regression models (data not shown).

Discussion

In the present study, we have identified that both *LMO3* and *HEN2* are expressed at higher levels in aggressive neuroblastomas especially with *MYCN* amplification than those with favorable prognosis. Coexpression of *LMO3* and *HEN2* has been observed almost exclusively in neuroblastoma cell lines, not the other lines, suggesting that their expression and function are neuronal specific. Furthermore, LMO3 physically interacted with HEN2 in mammalian cells. The functional significance of LMO3 expression was shown by a stable transfection into SH-SY5Y neuroblastoma cells, colony formation in soft agar, and tumor growth in nude mice, all of which have suggested that LMO3, probably by interacting with endogenous HEN2, markedly promotes the tumor growth. Indeed, the tumors with high expression of both *LMO3* and *HEN2* have shown the worst prognosis in the analysis of 87 primary neuroblastomas. Thus, our results suggested that, in concert with HEN2, the neuronal specifically expressed LMO3 plays an important role in the tumorigenesis of neuroblastoma. Our observation is strikingly intriguing because that *LMO1* or *LMO2* is already known to be the oncogene in T-cell acute lymphoblastic leukemia and that *LMO4* has recently been implicated in the genesis of breast cancer (4, 9).

We have identified a *Nbla3267/LMO3* clone from the screening of differentially expressed genes between favorable and unfavorable subsets of neuroblastoma. *LMO3* was one of the genes expressed at higher levels in the latter than the former (24), like *MYCN* oncogene and *DDX1*, a DEAD box gene coamplified with *MYCN* in aggressive neuroblastomas. In the development of hematopoietic system, LMO1 and LMO2 form a transcriptional complex with Ldb1, a LIM domain–binding protein, and a basic helix-loop-helix protein TAL1, which was identified as an oncogene at the translocation breakpoint in T-cell ALL (4–7). From the analogy with the LMO1 or LMO2 transcriptional machinery in T-cell ALL, we searched for the similar complex in the neuronal system by using the different subsets of primary neuroblastoma and the cell lines in comparison with the T-cell ALL cell lines. As a result, the neuronal-specific pattern of expression was observed in *LMO3*, *Ldb2*, *HEN1*, and *HEN2*, among which *LMO3* and *HEN2* were significantly highly expressed in the unfavorable subset of neuroblastomas with *MYCN* amplification compared with the favorable subset. This result strongly suggested that *LMO3* may function in collaboration with *HEN2* in advanced stages of neuroblastoma. Indeed, both genes were coexpressed only in neuroblastoma derived-cell lines, not in other tumor-derived ones, suggesting that their expression is lineage specific. Furthermore, LMO3 and HEN2 physically interacted in mammalian cells, albeit with weak interaction between LMO3 and HEN1 (35). Thus, these results also suggest that LMO3 and HEN2 form a neuronal cassette mimicking the hematopoietic complex composed of LMO2 and TAL1 and regulate the growth of neuroblastoma.

The neuronal-specific basic helix-loop-helix transcription factors, HEN1 and HEN2, were originally identified from the cDNA library of a neuroblastoma cell line based on cross-hybridization with TAL1 (14, 15). Their expression was restricted to the developing nervous system and a neuroblastoma cell line. However, their function has long been unclear. Recently, Bao et al. have reported that HEN1 interacts with LMO proteins by yeast two-hybrid screen and that *Xenopus* HEN1, in concert with XLMO3, is a critical regulator of neurogenesis (35). This prompted us to test our hypothesis both *in vitro* and *in vivo*. As the results, we found that the SH-SY5Y neuroblastoma cells stably overexpressing LMO3, presumably by acting with endogenous HEN2, gained rapid cell growth in the culture medium with 10% or 1% serum, in the soft agar medium, and in nude mice. These suggested that LMO3 is a neuronal-specific oncogene in neuroblastoma, without any rearrangement of the *LMO3* gene (data not shown). However, we failed to establish a stable SH-SY5Y cell line transfected with HEN2. It is presumed that overexpression of HEN2 might have caused cell death or growth arrest in the cells, albeit the reason is elusive.

The double transgenic mice overexpressing LMO2 and TAL1 displayed a more rapid development of leukemia compared with those overexpressing LMO2 alone, suggesting that LMO2 and TAL1 act synergistically through their complex formation in the development of leukemia (13). Of note, Ono et al. reported that LMO2 and TAL1 act as cofactors for GATA3 to induce the expression of the *retinaldehyde dehydrogenase 2* gene in T-cell ALL (39). On the other hand, a stable complex comprising LMO2, TAL1, and GATA1 was required to promote erythroid differentiation (32). Therefore, LMO3 and HEN2 may also form a nuclear complex, including family members of GATA to regulate cell growth and differentiation in neuroblastoma. Our preliminary data have suggested that GATA2, GATA3, GATA4, and GATA6 are highly expressed in neuroblastoma cell lines, among which GATA4 and GATA6 are predominantly coexpressed in neuroblastoma cell lines compared with T-cell ALL lines. Thus, LMO3 and HEN2, in collaboration with GATA and Ldb families, may play a role in determining cell fate in both neural development and neuroblastoma genesis, although this hypothesis needs to be elucidated. Recently, it has been shown that LMO3 enhanced the ability of HEN1 through the physical interaction to transactivate the expression of *Neurogenin-1* as well as *NeuroD* and thereby induced the neuronal differentiation in frog embryos (35). We tested if this is the case in the neuroblastoma cells. However, our preliminary results suggested that the LMO3/HEN2 complex does not transactivate the *Neurogenin-1* as well as *NeuroD* promoter in neuroblastoma cell lines,[5] although it is unclear if the complex could work in normal neuronal development. Thus, like LMO2, alterations in the LMO3-containing transcriptional complex might differentially regulate expression of the downstream target genes closely involved in neuronal differentiation or tumor formation.

[5] Unpublished data.

It is striking that high levels of expression of both *LMO3* and *HEN2* are significantly associated with the poor prognosis in primary neuroblastomas. This clearly reflects how importantly both genes are functioning in the progression of neuroblastoma *in vivo*. Of interest, expression of either gene is well correlated with *MYCN* amplification, raising the possibility that they might be the downstream targets of MYCN. However, we could not confirm it in human neuroblastoma cell line SH-EP in which MYCN was regulated under the control of the rTet-inducible expression system (40). In agreement with this, cDNA microarray-based screening for the genes induced in the *MYCN*-amplified neuroblastoma cells thus far failed to detect either LMO3 or HEN2 (41, 42). The link between LMO family molecules and the other oncogenes or tumor suppressor genes is also important. Despite the lack of prognostic significance, LMO4 overexpressed in breast cancer seems to be indispensable in the mammary carcinogenesis because it interacts with both BRCA1 and CtIP to repress the BRCA1 function (10). This suggests that, similarly to LMO4, LMO3 may also have the interacting partners related to the tumorigenesis. Thus, LMO3 and HEN2 as well as their associated molecules might be good candidates for the future targets of the therapy against aggressive neuroblastomas.

Acknowledgments

Received 12/28/2004; revised 3/9/2005; accepted 3/23/2005.

Grant support: Grant-in-Aid from the Ministry of Health, Labour and Welfare for Third Term Comprehensive Control Research for Cancer, Grant-in-Aid for Scientific Research on Priority Areas from the Ministry of Education, Culture, Sports, Science and Technology, Japan, and Grant-in-Aid for Scientific Research from Japan Society for the Promotion of Science. M. Aoyama is an awardee of the Research Resident Fellowship from the Foundation for Promotion of Cancer Research in Japan.

The costs of publication of this article were defrayed in part by the payment of page charges. This article must therefore be hereby marked *advertisement* in accordance with 18 U.S.C. Section 1734 solely to indicate this fact.

We thank S. Sakiyama for critical reading of the article; A. Morohashi, N. Kitabayashi, H. Murakami, and N. Sugimitsu for excellent technical assistance; and the following institutions and hospitals for supplying the tumor samples: Department of Pediatric Surgery, Iwaki Kyoritsu Hospital; Departments of Pediatrics and Pediatric Surgery, Aichi Medical University; Department of Pediatrics, Nara Hospital; Department of Pediatrics, Kyoto Prefectural University of Medicine; Department of Pediatric Surgery, Kimitsu Central Hospital; Department of Surgery, Gunma Children's Medical Center; Department of Pediatrics, Sapporo National Hospital; Departments of Pediatrics, Pediatric Surgery, and General Surgery, Jichi Medical School; Departments of Pediatrics and Pediatric Surgery, Kagoshima University; Department of Pediatrics, Juntendo University; Department of Pediatric Surgery, Showa University; Department of Pediatric Surgery, Niigata University; Departments of Surgery and Pathology, Chiba Children's Hospital; Department of Pediatric Surgery, Chiba University; Department of Pediatric Surgery, Osaka City General Hospital; Department of Pediatric Surgery, Tsukuba University; Department of Pediatric Surgery, Tokai University; Department of Surgery, Tokyo Metropolitan Kiyose Children's Hospital; Department of Pediatric Surgery, Tohoku University; Tomor Board, Hyogo Prefectural Kobe Children's Hospital; and First Department of Surgery, Hokkaido University.

References

1. Dawid IB, Breen JJ, Toyama R. LIM domains: multiple roles as adaptors and functional modifiers in protein interactions. Trends Genet 1998;14:156–62.
2. Sanchez-Garcia I, Rabbitts TH. The LIM domain: a new structural motif found in zinc-finger-like proteins. Trends Genet 1994;10:315–20.
3. Dawid IB, Toyama R, Taira M. LIM domain proteins. C R Acad Sci III 1995;318:295–306.
4. Rabbitts TH. LMO T-cell translocation oncogenes typify genes activated by chromosomal translocations that alter transcription and developmental processes. Genes Dev 1998;12:2651–7.
5. McGuire EA, Rintoul CE, Sclar GM, Korsmeyer SJ. Thymic overexpression of Ttg-1 in transgenic mice results in T-cell acute lymphoblastic leukemia/lymphoma. Mol Cell Biol 1992;12:4186–96.
6. Fisch P, Boehm T, Lavenir I, et al. T-cell acute lymphoblastic lymphoma induced in transgenic mice by the RBTN1 and RBTN2 LIM-domain genes. Oncogene 1992;7:2389–97.
7. Neale GA, Rehg JE, Goorha RM. Disruption of T-cell differentiation precedes T-cell tumor formation in LMO-2 (rhombotin-2) transgenic mice. Leukemia 1997;3:289–90.
8. Kenny DA, Jurata LW, Saga Y, Gill GN. Identification and characterization of LMO4, an LMO gene with a novel pattern of expression during embryogenesis. Proc Natl Acad Sci U S A 1998;95:11257–62.
9. Visvader JE, Venter D, Hahm K, et al. The LIM domain gene LMO4 inhibits differentiation of mammary epithelial cells *in vitro* and is overexpressed in breast cancer. Proc Natl Acad Sci U S A 2001;98:14452–7.
10. Sum EY, Peng B, Yu X, et al. The LIM domain protein LMO4 interacts with the cofactor CtIP and the tumor suppressor BRCA1 and inhibits BRCA1 activity. J Biol Chem 2002;277:7849–56.
11. Foroni L, Boehm T, White L, et al. The rhombotin gene family encode related LIM-domain proteins whose differing expression suggests multiple roles in mouse development. J Mol Biol 1992;226:747–61.
12. Wadman I, Li J, Bash RO, et al. Specific *in vivo* association between the bHLH and LIM proteins implicated in human T cell leukemia. EMBO J 1994;13:4831–9.
13. Larson RC, Lavenir I, Larson TA, et al. Protein dimerization between Lmo2 (Rbtn2) and Tal1 alters thymocyte development and potentiates T cell tumorigenesis in transgenic mice. EMBO J 1996;15:1021–7.
14. Brown L, Espinosa R III, Le Beau MM, Siciliano MJ, Baer R. HEN1 and HEN2: a subgroup of basic helix-loop-helix genes that are coexpressed in a human neuroblastoma. Proc Natl Acad Sci U S A 1992;89:8492–6.
15. Begley CG, Lipkowitz S, Gobel V, et al. Molecular characterization of NSCL, a gene encoding a helix-loop-helix protein expressed in the developing nervous system. Proc Natl Acad Sci U S A 1992;89:38–42.
16. Brodeur GM, Azar C, Brother M, et al. Effect of genetic factors on prognosis and treatment. Cancer 1992;70:1685–94.
17. Brodeur GM, Nakagawara A. Molecular basis of clinical heterogeneity in neuroblastoma. J Pediatr Hematol Oncol 1992;14:111–6.
18. Brodeur GM, Seeger RC, Schwab M, Varmus HE, Bishop JM. Amplification of N-*myc* in untreated human neuroblastomas correlates with advanced disease stage. Science 1984;224:1121–4.
19. Seeger RC, Brodeur GM, Sather H, et al. Association of multiple copies of the N-*myc* oncogene with rapid progression of neuroblastomas. N Engl J Med 1985;313:1111–6.
20. Nakagawara A, Arima M, Azar CG, Scavarda NJ, Brodeur GM. Inverse relationship between trk expression and N-*myc* amplification in human neuroblastomas. Cancer Res 1992;52:1364–8.
21. Nakagawara A, Arima-Nakagawara M, Scavarda NJ, Azar CG, Cantor AB, Brodeur GM. Association between high levels of expression of the TRK gene and favorable outcome in human neuroblastoma. N Engl J Med 1993;328:847–54.
22. Gross N, Beretta C, Peruisseau G, Jackson D, Simmons D, Beck D. CD44H expression by human neuroblastoma cells: relation to MYCN amplification and lineage differentiation. Cancer Res 1994;54:4238–42.
23. Berwanger B, Hartmann O, Bergmann E, et al. Loss of a FYN-regulated differentiation and growth arrest pathway in advanced stage neuroblastoma. Cancer Cell 2002;2:377–86.
24. Ohira M, Morohashi A, Inuzuka H, et al. Expression profiling and characterization of 4200 genes cloned from primary neuroblastomas: identification of 305 genes differentially expressed between favorable and unfavorable subsets. Oncogene 2003;22:5525–36.
25. Ohira M, Shishikura T, Kawamoto T, et al. Hunting the subset-specific genes of neuroblastoma: expression profiling and differential screening of the full-length-enriched oligo-capping cDNA libraries. Med Pediatr Oncol 2000;35:547–9.
26. Brodeur GM, Pritchard J, Berthold F, et al. Revisions of the international criteria for neuroblastoma diagnosis, staging, and response to treatment. J Clin Oncol 1993;11:1466–77.
27. Matsumura T, Iehara T, Sawada T, Tsuchida Y. Prospective study for establishing the optimal therapy of infantile neuroblastoma in Japan. Med Pediatr Oncol 1998;31:210.
28. Kaneko M, Nishihira H, Mugishima H, et al.; Study Group of Japan for Treatment of Advanced Neuroblastoma, Tokyo, Japan. Stratification of treatment of stage 4 neuroblastoma patients based on N-*myc* amplification status. Med Pediatr Oncol 1998;31:1–7.
29. Takihara Y, Tomotsune D, Shirai M, et al. Targeted disruption of the mouse homologue of the *Drosophila* polyhomeotic gene leads to altered anteroposterior patterning and neural crest defects. Development 1997;124:3673–82.
30. Agulnick AD, Taira M, Breen JJ, Tanaka T, Dawid IB, Westphal H. Interactions of the LIM-domain-binding factor Ldb1 with LIM homeodomain proteins. Nature 1996;384:270–2.
31. Jurata LW, Kenny DA, Gill GN. Nuclear LIM interactor, a rhombotin and LIM homeodomain interacting protein, is expressed early in neuronal development. Proc Natl Acad Sci U S A 1996;93:11693–8.
32. Bach I, Carriere C, Ostendorff HP, Andersen B, Rosenfeld MG. A family of LIM domain-associated cofactors confer transcriptional synergism between LIM and Otx homeodomain proteins. Genes Dev 1997;11:1370–80.
33. Osada H, Grutz G, Axelson H, Forster A, Rabbitts TH. Association of erythroid transcription factors: complexes involving the LIM protein RBTN2 and the zinc-finger protein GATA1. Proc Natl Acad Sci U S A 1995;92:9585–9.
34. Valge-Archer VE, Osada H, Warren AJ, et al. The LIM protein RBTN2 and the basic helix-loop-helix protein TAL1 are present in a complex in erythroid cells. Proc Natl Acad Sci U S A 1994;91:8617–21.
35. Bao J, Talmage DA, Role LW, Gautier J. Regulation of neurogenesis by interactions between HEN1 and neuronal LMO proteins. Development 2000;127:425–35.

36. Ono Y, Fukuhara N, Yoshie O. Transcriptional activity of TAL1 in T cell acute lymphoblastic leukemia (T-ALL) requires RBTN1 or -2 and induces TALLA1, a highly specific tumor marker of T-ALL. J Biol Chem 1997;272: 4576–81.
37. Aplan PD, Jones CA, Chervinsky DS, et al. An scl gene product lacking the transactivation domain induces bony abnormalities and cooperates with to generate T-cell malignancies in transgenic mice. EMBO J 1997;16:2408–19.
38. Eggert A, Grotzer MA, Ikegaki N, Liu XG, Evans AE, Brodeur GM. Expression of the neurotrophin receptor TrkA down-regulates expression and function of angiogenic stimulators in SH-SY5Y neuroblastoma cells. Cancer Res 2002;62:1802–8.
39. Ono Y, Fukuhara N, Yoshie O. TAL1 and LIM-only proteins synergistically induce retinaldehyde dehydrogenase 2 expression in T-cell acute lymphoblastic leukemia by acting as cofactors for GATA3. Mol Cell Biol 1998;18:6939–50.
40. Lutz W, Stohr M, Schurmann J, Wenzel A, Lohr A, Schwab M. Conditional expression of N-*myc* in human neuroblastoma cells increases expression of α-prothymosin and ornithine decarboxylase and accelerates progression into S-phase early after mitogenic stimulation of quiescent cells. Oncogene 1996;13:803–12.
41. Schuldiner O, Benvenisty N. A DNA microarray screen for genes involved in c-MYC and N-MYC oncogenesis in human tumors. Oncogene 2001;20:4984–94.
42. Shohet JM, Hicks MJ, Plon SE, et al. Minichromosome maintenance protein MCM7 is a direct target of the MYCN transcription factor in neuroblastoma. Cancer Res 2002;62:1123–8.

Clinical significance of serum NM23-H1 protein in neuroblastoma

Junko Okabe-Kado,[1,4] Takashi Kasukabe,[1] Yoshio Honma,[1] Ryoji Hanada,[2] Akira Nakagawara[3] and Yasuhiko Kaneko[1]

[1]Research Institute for Clinical Oncology, Saitama Cancer Center, 818 Komuro, Ina-machi, Kitaadachi-gun, Saitama 362-0806; [2]Saitama Children's Medical Center, 2100 Magome, Iwatsuki, Saitama 339-8551; and [3]Department of Biochemistry, Chiba Cancer Center Research Institute, 666-2 Nitona-cho, Chuo-ku, Chiba 260-8717, Japan

(Received April 28, 2005/Revised July 1, 2005/Accepted July 4, 2005/Online publication August 29, 2005)

We have previously reported that *NM23* genes are overexpressed in various hematological malignancies and that serum NM23-H1 protein levels are useful for predicting patient outcomes. In this study we assessed the clinical implications of serum NM23-H1 protein on neuroblastoma. We examined serum NM23-H1 protein levels in 217 patients with neuroblastoma, including 131 found by mass-screening and 86 found clinically by an enzyme-linked immunosorbent assay, and determined the association between levels of this protein, and known prognostic factors or the clinical outcome. The serum NM23-H1 protein level was higher in neuroblastoma patients than in control children ($P < 0.0001$). Patients with *MYCN* amplification had higher serum NM23-H1 levels than those with a single copy of *MYCN*. Overall survival was assessed in the 86 patients found clinically, and was found to be worse in patients with higher serum NM23-H1 levels (≥ 250 ng/mL) than in those with lower levels (< 250 ng/mL; $P = 0.034$). The higher level of NM23-H1 was correlated with a worse outcome in patients with a single *MYCN* copy, or in those younger than 12 months of age. Serum NM23-H1 protein levels may contribute to predictions of clinical outcome in patients with neuroblastoma. (*Cancer Sci* 2005; 96: 653–660)

The *NM23* gene was identified by differential hybridization of a cDNA library with total RNA extracted from slightly and highly metastatic melanoma cell lines.[1] The *NM23* gene has been identified as a family of genes encoding different isoforms of nucleoside diphosphate kinase (NDPK).[2] *NM23* genes play critical roles in cellular proliferation, differentiation, oncogenesis, and tumor metastasis.[1,3] The mechanisms for these pleiotropic effects are not well understood. Eight isotypes of the human *NM23* gene (*NM23-H1*, *NM23-H2*, *NM23-H3/DR-NM23*, *NM23-H4*, *NM23-H5*, *NM23-H6*, *NM23-H7*, and *NM23-H8*) have been identified.[2] Among these, only *NM23-H1* and *NM23-H2* have been studied extensively in human cancers.

The level of *NM23-H1* expression is inversely correlated with the tumor's metastatic potential in experimental rodent cells and in human tumors such as breast, ovarian, cervical and gastric cancer, hepatocellular carcinoma, and melanomas.[4] Therefore, *NM23-H1* is implicated in the regulation of metastasis in a variety of human cancers. However, overexpression of the *NM23-H1* gene has been reported in various neoplasms including neuroblastoma, hematological malignancies, and pancreatic, lung, ovarian and gastric cancers.[5–8] Overexpression of *NM23-H1* is indicative of a poor patient prognosis for patients with neuroblastoma, acute myelogenous leukemia (AML), or non-Hodgkin's lymphoma (NHL).[8–10]

In neuroblastoma, a gain of 17q is the most frequent genetic abnormality, followed by 1p deletion and *MYCN* amplification, both of which correlate closely with 17q gain. The three genetic events are strong predictors of unfavorable prognosis.[11,12] The *NM23* genes are located at the edge of the common chromosomal region of 17q gain. Godfrid *et al.* identified genes that are activated in the *MYCN* downstream pathway using SAGE libraries of *MYCN*-transfected and control neuroblastoma cell lines.[13] The *NM23-H1* and *NM23-H2* genes are strongly induced in *MYCN*-expressing cells. Neuroblastoma tumor and cell line panels reveal a striking correlation between *MYCN* amplification and mRNA or protein expression of both *NM23* genes. These findings suggest that *NM23-H1* and *NM23-H2* expression may be increased by 17q gain in neuroblastoma, and can be further upregulated by *MYCN* overexpression. These observations suggest a role of *NM23-H1* and *NM23-H2* in the tumorigenesis of an unfavorable type of neuroblastoma.

We previously established an enzyme-linked immunosorbent assay (ELISA) technique for determining the serum level of NM23-H1 protein.[14] Serum levels of NM23-H1 in patients with NHL and AML are significantly higher than those in controls, and elevated NM23-H1 levels correlate with poor prognosis in these patients.[10,15] It has been strongly suggested that serum NM23-H1 protein is produced directly by tumor cells and its level depends on the total mass of malignant cells overexpressing *NM23-H1*.[14,16] These results indicate that the serum level of NM23-H1 protein may be clinically useful as a prognostic factor in NHL and AML. The present study assessed the clinical implications of serum NM23-H1 protein levels in patients with neuroblastoma, in whom tumor samples were used to determine the biological prognostic factors.

Materials and Methods

Patients and controls

Serum NM23-H1 protein was measured in 217 untreated neuroblastoma patients who were admitted to various institutions in Japan and underwent biopsy or surgery between 2000 and 2002. The 217 patients included 131 who were found by

[4]To whom correspondence should be addressed.
E-mail: jkado@cancer-c.pref.saitama.jp

 doi: 10.1111/j.1349-7006.2005.00091.x

a mass-screening (MS) program for infants at 6 months of age by measuring urinary catecholamine metabolites and 86 who were found clinically.[17] Of the 86 patients, 29 who were younger than 12 months old were mostly found before MS, and 57 who were 12 months old or older underwent MS with a negative result, or did not undergo MS. Patients were staged according to the International Neuroblastoma Staging System (INSS).[18] Patients of any age with stage 1 or 2 disease, and those younger than 12 months of age with stage 3 disease were treated by surgery or surgery and chemotherapy consisting of cyclophosphamide and vincristine; patients 12 months or older with stage 3 or stage 4 disease and those younger than 12 months of age with stage 4 disease were treated according to the protocol published by the Japanese Neuroblastoma Study Group.[19] Serum samples from 23 children consisting of 22 with inguinal hernias and one with an edematous scrotum before surgery were analyzed for comparison. The median age of the children was 23 months (range: 3–49 months). Informed consent was obtained from patients and/or their parents, and the ethics committee of Saitama Cancer Center approved the study design.

Venous blood samples

Peripheral venous blood samples were collected in sterile test tubes with heparin and placed on ice. The samples were centrifuged at 2000*g* for 15 min at 4°C, and stored at −20°C. As a marker of hemolysis, free serum hemoglobin (Hb) was determined according to the method of Testa *et al.*[20]

ELISA for human NM23-H1 protein

NM23-H1 protein levels in serum were determined using a sandwich ELISA assay, as described previously.[14,15] Recombinant NM23-H1-GST protein was used as a standard.

Examination of *MYCN* copy number, TRKA expression and ploidy

DNA preparation, digestion, and Southern blot analysis using the *MYCN* probe were carried out as described previously.[12] The presence of more than three copies of the *MYCN* gene per haploid genome was considered to indicate amplification.[21] *TRKA* expression was examined by northern blotting as reported previously.[22] DNA index was analyzed on a Becton-Dickinson FACScan flow cytometer by DNA cell-cycle analysis software (version C).

Statistical analysis

The significance of differences in various clinical and biological aspects of the disease among the patient groups was examined by using the Mann–Whitney *U* or Kruskal–Wallis test (non-parametric analysis). Spearman's correlation coefficient (rs) by ranks was used to evaluate the correlation between paired values. Survival analysis was performed according to the Kaplan–Meier method, and the significance of differences in survival was determined by using the generalized Wilcoxon's and log-rank tests. A multivariate analysis of prognostic factors was performed using Cox's proportional-hazards regression model. All statistical analyses were performed with Excell Statcel and Stat Flex software (version 5.0, Artech Co. Ltd, Osaka, Japan), and $P < 0.05$ was taken to indicate significance.

Results

Examination of serum NM23-H1 protein levels in neuroblastoma patients and control children

The serum level of NM23-H1 was examined in 217 neuroblastoma patients and 23 control children. The serum levels of NM23-H1 were significantly higher in patients with neuroblastoma ($n = 217$, mean ± SD 176 ± 280 ng/mL) than in the control children ($n = 23$, 27 ± 41 ng/mL, $P < 0.0001$; Fig. 1a). The serum NM23-H1 levels of the control children were higher than those of the healthy adults (data not shown). The serum NM23-H1 levels in patients with neuroblastoma were significantly higher than those in patients with various hematological malignancies (data not shown). Next, the relationship between serum levels of NM23-H1 and Hb was examined in 217 neuroblastoma patients and 23 control children, because the NM23-H1 protein leaked from red blood cells by hemolysis may have elevated the serum NM23-H1 levels.[23] The results showed a weak correlation (rs = 0.3958, $P = 7.5356 \times 10^{-10}$, Spearman's correlation coefficient by ranks), although some patients had a higher Hb level but a lower NM23-H1 level, or a lower Hb level but a higher NM23-H1 level (Fig. 1b). When we chose samples from 156 patients

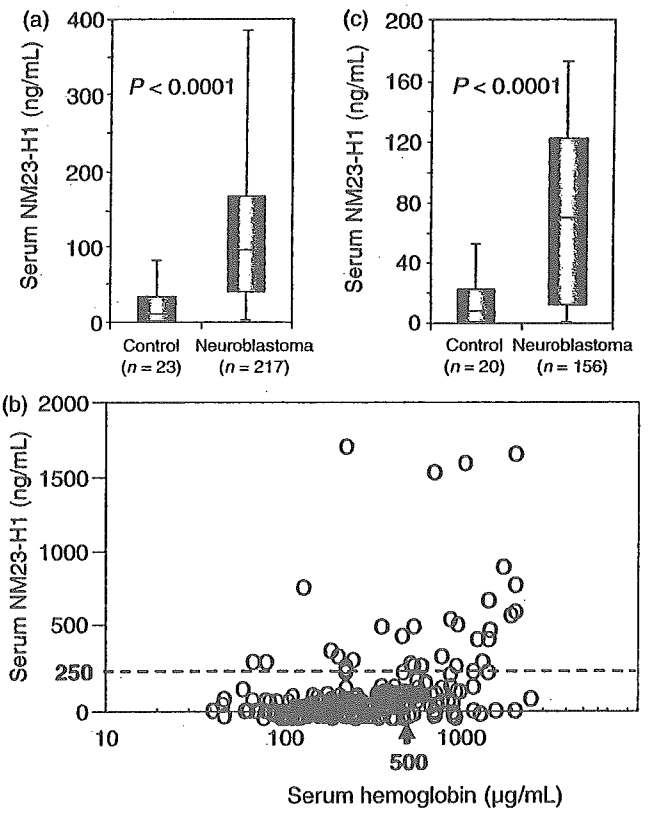

Fig. 1. Serum NM23-H1 levels in patients with neuroblastoma and in control children. (a) Box plots of NM23-H1 serum levels for 217 patients with neuroblastoma and 23 control children with any serum hemoglobin levels. (b) Relationship between the serum levels of NM23-H1 and hemoglobin in all samples examined (black circles, neuroblastoma patients [$n = 217$]; red circles, control children [$n = 23$]). (c) Box plots of NM23-H1 serum levels for 156 patients with neuroblastoma and 20 control children with serum hemoglobin levels less than 500 μg/mL.

 doi: 10.1111/j.1349-7006.2005.00091.x

Table 1. Relationship between serum NM23-H1 protein levels and clinicopathological findings in 217 patients with neuroblastoma and 23 control children

Clinicopathological findings	Number of patients (mean ± SD)	Serum NM23-H1 (ng/mL)	*P*-value (analysis)
Control children	23	27 ± 41	
All patients	217	176 ± 280	< 0.0001 (MW)
Method of detection			
Mass-screening	131	135 ± 206	
Found clinically	86†	239 ± 357	0.0595 (MW)
Age of patients			
< 12 months	134	168 ± 292	
≥ 12 months	83	190 ± 260	0.2427 (MW)
Stage of the disease			
1 + 2 + 4s	122	136 ± 159	
3 + 4	95	227 ± 378	0.8088 (MW)
Primary site			
Mediastinum	31	145 ± 212	
Adrenal	101	187 ± 290	
Abdomen	78	184 ± 302	0.3393 (KW)
Others	7	74 ± 82	
MYCN copy number			
1	186	143 ± 204	
> 3	31	378 ± 519	0.0006 (MW)
TRKA expression	173		
Medium or high	125	150 ± 209	
None or low	48	238 ± 373	0.4629 (MW)
Ploidy	168		
Diploid	69	188 ± 273	
Hyperdiploid	99	185 ± 284	0.9012 (MW)
Others	7	112 ± 126	

MW, Mann–Whitney *U*-test; KW, Kruskal–Wallis test. †Table 2.

and 20 control children with serum Hb less than 500 μg/mL, the correlation between serum NM23-H1 and Hb levels was negligible (rs = 0.2351, $P = 0.0035$). Even in these patients, the serum levels of NM23-H1 were significantly higher (n = 156, 113 ± 184 ng/mL) than in the control children ($n = 20$, 20 ± 35 ng/mL, $P < 0.0001$; Fig. 1c).

Relationship between serum NM23-H1 protein levels and clinicopathological features in neuroblastoma

The relationship between serum NM23-H1 levels and various clinical and biological features in the 217 patients is shown in Table 1. The serum NM23-H1 levels tended to be higher in patients found clinically than in those found by MS ($P = 0.0595$), and were significantly higher in patients with amplified *MYCN* copies than in those with a single *MYCN* copy ($P = 0.0006$; Table 1). There was a correlation between *MYCN* amplification and the elevated serum NM23-H1 level (≥ 250 ng/mL) in all 217 patients (rs = 0.6970, $P = 0.0005$). However, serum Hb concentrations did not correlate with *MYCN* amplification ($P = 0.6320$), or other factors (data not shown). There was no significant difference in the serum NM23-H1 levels between two groups of patients classified by age of the patients, stage of the disease, expression levels of *TRKA*, or tumor cell ploidy (Table 1).

Serum NM23-H1 levels and overall survival

Of the 217 patients, the 86 patients who were found clinically were included and the 131 patients found by MS were excluded from survival analysis, because all the 131 patients were alive at the last follow-up (18–51 months), and the clinical and biological features are different for the patients found by MS and those found clinically.[12] The relationship between serum NM23-H1 levels and various clinical and biological features in the 86 patients was similar to that found for all 217 patients (Tables 1, 2). The 86 patients were divided into two groups according to various cut-off points over 100 ng/mL, which was the upper limit in control serum (mean + 2 × SD = 20 + 2 × 35 = 90). The cut-off points used here were 100 ng/mL (< 100, $n = 39$, *vs* ≥ 100, $n = 47$), 150 ng/mL (< 150, $n = 54$, *vs* ≥ 150, $n = 32$), 200 ng/mL (< 200, $n = 60$, *vs* ≥ 200, $n = 26$) and 250 ng/mL (< 250, $n = 64$, *vs* ≥ 250, $n = 22$). The cut-off value of greater than 250 ng/mL showed the most significant prognostic effects with generalized Wilcoxon's and log-rank test analysis (data not shown). Therefore, we used 250 ng/mL of serum NM23-H1 as a cut-off value. As shown in Figure 2a, patients with the higher serum NM23-H1 levels had worse overall survival than those with the lower levels ($P = 0.0219$ according to the generalized Wilcoxon test, $P = 0.0340$ according to the log-rank test). Overall survival was significantly worse for patients who were 12 months or older than for those younger than 12 months of age ($P = 0.0364$ and $P = 0.0158$), for patients at stages 3 and 4 than for those at stages 1, 2 and 4S ($P = 0.0157$ and $P = 0.0082$), and for patients with *MYCN* amplification than for those with a single copy of *MYCN* ($P = 0.0195$ and $P = 0.0054$; Fig. 2b,c,d). These results